Integrated Master in Environmental Engineering 2013/2014

Membranes with nanostructured materials for water desalination and purification

Master Thesis

of

Carla Manuela Pires Esteves

Dissertation

Developed at

Laboratory of Catalysis and Materials (LCM)

Supervisors:

Adrián Manuel Tavares da Silva

Sergio Morales Torres

José Luís Cabral da Conceição Figueiredo

Department of Chemical Engineering

July 2014

Acknowledgements

I would like to express my deep gratitude to Sergio Morales Torres (Postdoctoral Researcher in FEUP), for his guidance, patience and useful elucidations during all last months. Your friendship, courage and motivation were indispensable to me throughout the work.

I am also grateful to my supervisor, Doctor Adrián Manuel Tavares da Silva, for all their useful and constructive recommendations on this project.

Words of appreciation to Professor José Luís Figueiredo, director of LCM, for given me the opportunity to work in this laboratory in order to accomplish all results in the work.

I also thanks all the members of the LCM team for the welcome in the group and all the help provided during this period, especially to Tânia L. dos Santos Silva and to Luisa M. Pastrana Martínez for all the help, support and total availability given.

Finally, the most important person for me, Joel Ribeiro, because you accompanied me and you are always there to help me.

Financial support for this work was provided by projects PTDC/AAC-AMB/122312/2010 co-financed by FCT (Fundação para a Ciência e a Tecnologia) and FEDER (Fundo Europeu de Desenvolvimento Regional) through Programme COMPETE (FCOMP-01-0124-FEDER-019503). This work was also partially co-financed by FCT and FEDER through project PEst-C/EQB/LA0020/2013 (COMPETE), and by QREN, ON2 (Programa Operacional do Norte) and FEDER through project NORTE-07-0162-FEDER-000050. Professor Luis Manuel Ferreira Melo is also acknowledged for kindly providing the equipment for contact angle determinations.

Resumo

No século XXI, o abastecimento de água para consumo tornou-se escasso, e as suas fontes naturais estão a diminuir. A dessalinização da água do mar e das águas salobras pode constituir uma excelente solução para o problema. A osmose direta (OD) é um processo promissor de dessalinização, já que é bastante económico e respeita o meio ambiente. No entanto, este processo apresenta duas limitações intrínsecas: o efeito da polarização por concentração e a incrustação da membrana. As membranas com compósito de película fina (TFC – *thin film composite*) são amplamente utilizadas no processo de OD e são constituídas por uma camada de poliamida ativa sobre um substrato, que geralmente é uma membrana de polisulfona (PS). A modificação das membranas com base de polisulfona feita com materiais nanoestruturados tem como objetivo aumentar a sua eficiência e, assim, minimizar os efeitos negativos associados ao processo de OD.

Membranas de PS com nanotubos de carbono (CNTs), óxido de grafeno (GO) e materiais compósitos de carbono-TiO_2 foram preparadas pelo método da inversão de fase e estudaram-se diferentes parâmetros de síntese, tais como a quantidade de material e a adição de um formador de poros (PVP – polivinilpirrolidona). De forma geral a adição de materiais nanoestruturados nas membranas de PS produz um aumento da porosidade e do ângulo de contato, em relação à membrana pura de PS. A utilização de PVP nas membranas puras de PS promove a formação de poros com maiores dimensões, enquanto que as membranas com TFC apresentam uma diminuição da porosidade e ângulo de contato em relação à membrana com suporte de PS correspondente.

Todas as membranas foram testadas em filtração, com água destilada e água salgada (C = 1000 ppm NaCl). O aumento da pressão transmembranar induz um maior fluxo de água. A membrana preparada com 0.1% de nanotubos de carbono originais (0.1MWp/PS) apresenta o fluxo de água mais elevado (18760 L h^{-1} m^{-2}) com água salgada. Contudo, neste processo a rejeição de sal para as membranas de PS foi na ordem dos 8%. Por seu lado, as membranas com TFC apresentam menor fluxo de água mas a rejeição de sal é mais elevada, comparativamente com as correspondentes membranas de PS. A membrana 0.1MWf/PS (com 0.1% de nanotubos de carbono funcionalizados) é aquela que apresenta melhores fluxos de água e rejeição de sal.

No processo de OD as membranas com TFC foram testadas com água destilada e 0.6 M de NaCl como solução de alimentação e de permeado, respetivamente. Obtêm-se geralmente fluxos mais elevados quando a membrana se coloca com a camada ativa voltada para o

permeado (ALDS - *active layer faced draw solution*). A melhor membrana com TFC testada em OD foi preparada com uma base de PS composta com 0.6% em massa do compósito de óxido de grafeno e TiO_2 (0.6GOT/PS-P_TFC), para a qual se obteve um fluxo de água de 12.1 L h^{-1} m^{-2} e uma rejeição de sal de 99%. Esta membrana foi também testada com outras soluções de permeado, sendo que se obteve um aumento do fluxo de água e do fluxo inverso de soluto quando a concentração do permeado foi 1.2 M NaCl, enquanto que ao usar uma solução de 1.25 M de $MgSO_4$ no permeado se verifica uma diminuição de ambos os parâmetros.

Palavras-passe: *Nanotubos de carbono, óxido de grafeno, materiais compósitos de carbono-TiO_2, membranas, osmose direta.*

Abstract

In the XXI century, the supply of drinking water is becoming scarce and the desalination of seawater offers an excellent solution to solve it. Forward osmosis (FO) is a promising desalination process because of its environmental friendly characteristics and low energy costs. However, it presents two intrinsic limitations: internal concentration polarization and membrane fouling. Thin film composite (TFC) membranes are widely used in FO and are composed of an active polyamide layer on a substrate. This substrate is typically a polysulfone (PS) membrane. The modification of PS substrates with nanostructured materials has as mission to increase the efficiency of the TFC membranes and overcome the problems of the FO process.

PS membranes blended with carbon nanotubes (CNTs), graphene oxide (GO) and carbon-TiO_2 composites were prepared by the phase inversion method, studying different synthesis parameters, such as material loading and addition of a pore former. In general, the addition of nanostructured material in the PS membranes produced an increase of both porosity and contact angle in comparison to the neat PS membrane. Pore formers produced membranes with larger pore sizes than those of the neat PS membrane, while TFC membranes presented a decrease of the porosity and the contact angle compared to the corresponding PS support.

All membranes were tested in filtration of DI water and slightly salty water. The increase of the trans-membrane pressure produced a higher water flux. The membrane prepared with 0.1 wt.% of pristine CNTs (0.1MWp/PS) presented the highest water flux (18760 L h^{-1} m^{-2}) with slightly salty water. However, the salt rejection of the PS membranes was near 8%. TFC membranes showed lower water flux but higher salt rejection compared to their corresponding PS supports. The 0.1MWf/PS membrane (with 0.1 wt.% of functionalized CNTs) has the highest water flux and salt rejection.

TFC membranes were tested in FO with DI water and 0.6 M NaCl as feed and draw solutions. A higher water flux was generally obtained when performing in active layer faced draw solution (ALDS) configuration. The most active TFC membrane in FO was that prepared on a PS membrane with 0.6 wt.% of a graphene oxide-TiO_2 composite (0.6GOT/PS-P_TFC), a water flux of 12.1 L h^{-1} m^{-2} and a salt rejection of 99% being obtained. This membrane was also tested with other draw solutions, an increase of both water flux and solute flux being observed with 1.2 M NaCl draw solution and a decrease of both parameters with 1.25 M $MgSO_4$ draw solution.

Keywords*: Carbon nanotubes, graphene oxide, carbon-TiO_2 composites, membranes, forward osmosis.*

Table of Contents

List of Tables

List of Figures

Abbreviations

ALDS	Active layer faced to the draw solution
ALFS	Active layer faced to the feed solution
CA	Cellulose acetate
CDI	Capacitive deionization
CNTs	Carbon nanotubes
DI	Deionized
ECP	External concentration polarization
ED	Electrodialysis
FCT	Fundação para a Ciência e a Tecnologia
FD	Freeze desalination
FEUP	Faculty of Engineering of University of Porto
FO	Forward osmosis
GO	Graphene oxide
GOT	Graphene oxide-titanium dioxide composite
ICP	Internal concentration polarization
IP	Interfacial polymerization
IPA	Isopropyl alcohol
LCM	Laboratory of Catalysis and Materials
LPD	Liquid phase deposition
LSRE	Laboratory of Separation and Reaction Engineering
MD	Membrane distillation
MED	Multi-effect distillation
MF	Microfiltration
MMM	Mixed matrix membrane
MPD	1,3-phenylendiamine
MSF	Multi-stage flash evaporation
MWCNTs	Multi-walled carbon nanotubes
MWf	Functionalized multi-walled carbon nanotubes
MWfT	Functionalized multi-walled carbon nanotubes-titanium dioxide composite

MWp	Pristine multi-walled carbon nanotubes
NF	Nanofiltration
NMP	1-methyl-2-pyrrolidinone
P25	Commercial bare titanium dioxide
PA	Polyamide
PAN	Polyacrylonitrile
PE	Polyethylene
PES	Polyethersulfone
PP	Polypropylene
PS	Polysulfone
PTFE	Polytetrafluoroethylene
PVDF	Polyvinylidene difluoride
PVP	Polyvinylpyrrolidone
RO	Reverse osmosis
SMEs	Small and medium enterprises
SWCNTs	Single-walled carbon nanotubes
TFC	Thin-film composite
TiO_2	Titanium dioxide
TMC	1,3,5-benzenetricarbonyl trichloride
TMP	Trans-membrane pressure
TPD	Temperature programmed desorption
UF	Ultrafiltration
VC	Vapour compression

Nomenclature

ρ_{IPA}	density of isopropyl alcohol	g cm^{-3}
ρ_p	density of polymer	g cm^{-3}
γ	surfasse tension coefficient	dynes cm^{-1}
θ	contact angle	°
A	area	m^2
C_f	feed concentration	g L^{-1}
C_d	draw concentration	g L^{-1}
C_p	permeate concentration	g L^{-1}
C_s	solute concentration	g L^{-1}
C_t	salt concentration at time *t*	g L^{-1}
d_{pore}	pore diameer	µm
J_s	reverse salt flux	g h^{-1} m^{-2}
J_w	water flux	L h^{-1} m^{-2}
m_d	weight of the dry membrane	g
m_w	weight of the wet membrane	g
M_w	molecular weight	g mol^{-1}
P_{bubble}	bubble pressure	bar
R	gas constant	L atm mol^{-1} K^{-1}
S_{BET}	surface area	m^2 g^{-1}
t	time	h
T	temperature	K
V	volume	m^3
V_p	pore volume	cm^3 g^{-1}
π	osmotic pressure	atm

1 Introduction

1.1 Introduction to the work plan

In recent decades, the exponential population growth, the water scarcity and the increasing demand for freshwater have forced small and medium enterprises (SMEs) and industry to search new methods capable to produce drinking water for both industrial and domestic usages [1]. This concern has motivated the development of sustainable technologies to obtain water with enough quality from different natural sources, including seawater.

During the last century, various technologies including adsorption, coagulation, flotation, ozonation, ion exchange as well as pressure-driven membrane filtration processes such as microfiltration (MF), ultrafiltration (UF), nanofiltration (NF) and reverse osmosis (RO), have been thoroughly investigated for water and wastewater treatment [2-4]. Some of these filtration processes, in particular RO, are also employed for desalination of brackish and sea water [5]. RO consists in the removal of salts, forcing a feed stream of water to pass across a semipermeable membrane by application of a high pressure [6] and, thereby, the process has a high energy consumption [7].

Among the different filtration processes involving the use of selective membranes, forward osmosis (FO) is gaining major attention since operates at zero or low hydraulic pressure and, thus, future challenges in water desalination can be overpassed with this process due to its low energy requirement and feasibility. Conceptually, FO is based on the osmotic pressure difference (i.e., chemical potential difference) between a feed solution and a concentrated solution [8], which is defined as draw solution. Besides the advantage of operating at zero or low hydraulic pressure, other unique characteristics of FO include a high water recovery rate [9], a low fouling and the possibility to avoid pre-treatment processes [10, 11]. One of the major drawbacks of FO is the internal concentration polarization (ICP), which reduces the osmotic pressure gradient across the active layer of the membrane and, consequently, the flux efficiency [12, 13]. ICP is a phenomenon caused by the hindered diffusion of solutes within the membrane support and occurs by the difference between the solute concentrations at the transverse boundaries of the support [14].

Filtration processes, including FO, require the use of semipermeable membranes, and thus market has been dominated by thin-film composite (TFC) membranes during decades, due to their prominent advantages such as a good separation efficiency, wide pH tolerance and

some specific features that can be controlled for each individual layer of the membrane [15, 16]. TFC membranes typically consist of two different layers: a substrate membrane (e.g., polysulfone) and an active polyamide layer, (dense, amorphous and very thin i.e. <0.2 μm) [17, 18].

Polysulfone-based membranes are widely used for water filtration and purification, due to their excellent heat resistance, chemical stability over a wide range of pHs. However, the polysulfone (PS) membranes have a hydrophobic nature and some desalination processes, such as FO requires membranes with appreciable hydrophilicity in order to enhance their productivity. In addition, the surface hydrophobicity is generally associated with the fouling of the membrane and, thus, with the membrane lifetime. The low permeability and the fouling of the membranes are often avoided with the increase of both surface hydrophilicity and porosity. In this way, the most widely employed method to increase the hydrophilicity of the membrane is to blend the PS polymer with a surface modifier or filler presenting hydrophilic characteristics, such as metal oxides, zeolites and, more recently, functionalized carbon materials [19, 20].

Among the mentioned materials, carbon nanotubes (CNTs) and graphene oxide (GO) have received increasing attention due to their unusual structural properties [21], chemical stability and the possibility to modify their surface chemistry by different oxidative treatments [22, 23]. The oxygen functional groups created allows improving the material solubility and facilitate its interaction with a variety of organic and inorganic materials, including polymers [24-26].

In this thesis, PS membranes blended with CNTs, GO and carbon-TiO_2 composites were prepared. Different synthesis parameters, such as material loading and addition of pore formers were studied. The performance of the membranes was first assessed in the filtration of deionized water and slightly salty water. The membranes with better efficiency were then used as supports for TFC membranes, which were tested in FO. The final goal was to design a membrane that presents high water flux (and as consequence lower energy consumption) and excellent salt rejection to be applied in the FO desalination technology.

1.2 Presentation of the Research Unit

The Laboratory of Catalysis and Materials (LCM) in partnership with the Laboratory of Separation and Reaction Engineering (LSRE), became a national Associate Laboratory in 2004, in

recognition of the capacity of the two units to cooperate in a stable, competent and effective way in the prosecution of specific objectives of the National Scientific and Technological Policy. The Associate Laboratory is hosted by the Faculty of Engineering of University of Porto (FEUP), a public institution of higher education with financial autonomy and the largest Faculty of the University of Porto.

The present work was performed in the framework of a LCM research topic (development of nanostructured materials) and under financial support of a FCT project, project (PTDC/AAC-AMB/122312/2010 – Carbon nanotube membranes for water desalination and purification). The work was carried out in the LCM laboratories located in the Department of Chemical Engineering/FEUP (E-301, E-302A and E-303). The most relevant equipments used in the present work were a stirred filtration cell, a prototype for the FO experiments, which was built and optimized in the framework of this MSc Thesis, and an ion chromatograph (Metrohm 881 Compact IC with sequential suppression).

1.3 Structure of the thesis

This thesis is divided into six chapters:

(i) The first chapter contextualizes the problem that is under investigation in this work and regards the main points discussed throughout the Thesis.

(ii) The state of art is presented in the second chapter, besides the theoretical fundamentals of the methods applied.

(iii) The detailed description of the materials prepared in this study as well as the characterizations performed are presented in the third chapter.

(iv) The results obtained during the project and their corresponding discussion are shown in the fourth chapter.

(v) The main conclusions resulting from this work are presented in chapter five.

(vi) The limitations encountered while performing the work are registered in the last chapter, together with some suggestions for future work.

2 State of the art, motivation and objectives

2.1 The desalination process

In developed countries, water is relatively inexpensive in comparison with many other regions of the world. However, the climatic change, population growth, scarcity of natural resources, water transport problems over long distances and the subsequent increase of the demand for water in arid, semiarid and coastal areas are contributing to an increasing interest in water desalination technologies as a way to increase the existing supplies. In addition, many communities are considering the desalting technologies as cost-effective methods to meet increasingly stringent water quality regulations [27]. The desalination process can be defined as the production of fresh water (i.e. with low concentration of dissolved salts) from seawater or other water sources [28], even those presenting salt concentrations larger than in seawater [29].

Desalination processes can be ordered into three categories regarding the associated separation mechanism: phase change, interaction with selective membranes and electrostatic interaction (Figure 1).

Figure 1: Types of desalination processes divided into three categories: phase change, interaction with selective membranes and electrostatic interactions.

The transformation of seawater to drinking water is the most widely recognized use of desalination technologies, although they are also used for improving the quality of water from brackish sources. Membrane desalting technologies are commonly used at home for the tap water treatment and for the treatment and recycling of domestic wastewater. They are also applied for industrial wastewater treatment, in order to recycle and produce high quality water for instance in pharmaceutical industries. Desalination processes are not only used to remove salts and other dissolved minerals from water, they are also used to separate pollutants, such as dissolved heavy metals, radionuclides, pathogens, arsenic, bacterial and dissolved organic matter [27].

In spite of the last twenty years, a significant reduction in power requirements, due to the improvement in flux and salt rejection, have been reached [27]. In this context, the increasing development of the established desalination technologies and mainly the research for membranes with finely-balanced characteristics are markedly justified.

2.2 The forward osmosis (FO) process

The osmosis phenomenon was discovered by Nollet in 1748 [30], and since then a few studies were conducted before a notorious progress on membrane-based technologies [31]. Nowadays, the interest on the osmosis phenomenon and thus on forward osmosis (FO) for water treatment, as alternative to other processes, has increased considerably [31]. FO has been even proposed for brine desalination, which has become a critical environmental concern in desalination plants, especially for inland communities where brine discharge sources are not always available [32].

In general, the desalination process by using FO involves two steps: (i) osmotic dilution of the draw solution and (ii) fresh water productions from the diluted draw solution. FO desalination processes can be classified into two types according to the final method for the water production. The first FO method employs thermolytic draw solutions, which are decomposed into volatile gases (e.g., CO_2 or SO_2) by heating after osmotic dilution. Thus, drinking water is recovered and the gases are recycled during the thermal decomposition. The another type of FO desalination process uses water-soluble salts or particles as draw solutes, fresh water being generated from the diluted draw solution by other separation methods [32].

In the FO process is not necessary to apply a pressure to the system, the water flows to the permeate side due to an osmotic pressure differential ($\Delta\pi$) across the membrane (Figure 2)

and caused by a concentrated solution (draw) [31]. Therefore, the water flows across the semi-permeable membrane from a saline stream (feed) towards a highly concentrated draw solution, diluting the draw solution and separating water from the saline feed water stream. The water would be subsequently extracted from the diluted draw solution by removing the solute in a subsequent step.

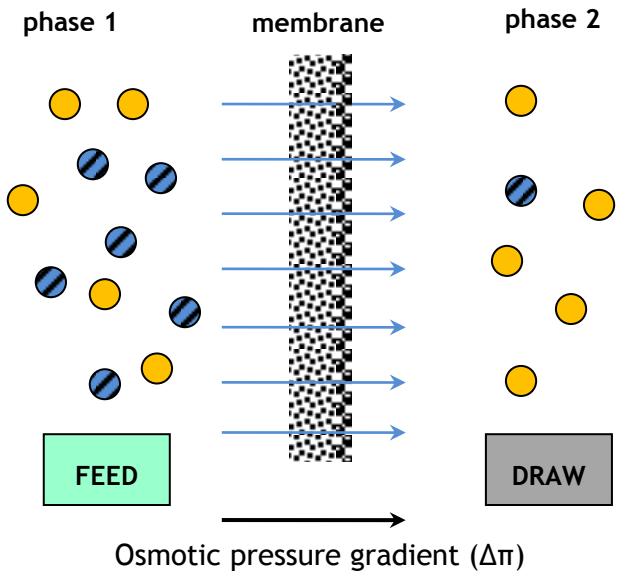

Figure 2: Schematic representation of FO desalination.

2.2.1 Osmotic pressure

Two solutions with different salt concentrations are separated by a selectively semipermeable membrane, in osmotically-driven membrane processes. This membrane allows the transport of water molecules only by rejecting most of the solute molecules or ions [33]. The difference between the concentration of the two solutions creates a gradient that drives water across the membrane from the low salt concentration side to the high salt concentration side. The water flow continues until the chemical potentials become equal on both sides of the membrane [34]. The osmotic pressure (π) arises as consequence of this concentration difference, and is equivalent to the pressure needed on the more concentrated solution to prevent the transport of water across the membrane [31]. A schematic illustration of this process is indicated in Figure 3 [35].

The osmotic pressure (π) can be defined by the van't Hoff equation (eq. 1) [31]:

$$\pi = \frac{C_s RT}{M_w} \qquad \textbf{(eq. 1)}$$

where C_s is the solute concentration (g L^{-1}), R is the gas constant (L atm mol^{-1} K^{-1}), T is the temperature (in K), and M_w is the molecular weight (g mol^{-1}) [31].

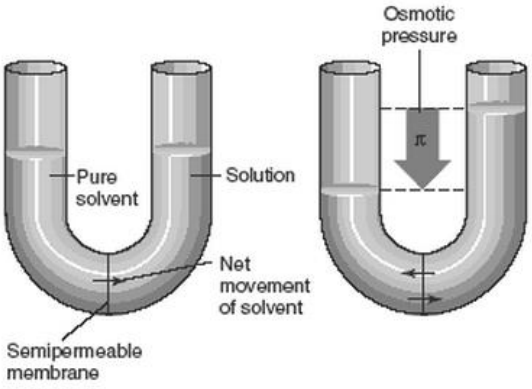

Figure 3: Scheme of the osmosis phenomenon and the osmotic pressure. Figure reprinted from [35].

According to eq. 1, the osmotic pressure is directly proportional to the solute concentration and inversely proportional to the molecular weight. In addition, if the solute dissociates (e.g., salts) or associates, a modification to the van't Hoff equation must be considered [31]. In this context, when solute dissociation occurs, the number of moles and consequently the osmotic pressure increase, while a decrease of the osmotic pressure occurs with the solute association and explained by the decrease of its number of moles. Substantial deviations from the van't Hoff law take place at high concentrations and with macromolecular solutions [36].

2.2.2 Concentration polarization and fouling

The flux into a membrane is largely influenced by both membrane intrinsic properties and fouling. For the FO process, the fouling may be complex due to the possible contribution of ICP, which is a phenomenon inherent of the osmosis-driven membrane processes and is due to hindered diffusion of solutes within the membrane support. In general, ICP diminishes the overall driving force across a membrane, but in some cases, it provides a self-compensating mechanism that could maintain relatively stable fluxes under fouling conditions [37].

The membrane orientation and the concentration of both feed and draw solutions have influence on the extent of ICP, fouling and flux stability [12, 13, 38]. In general, the concentration polarization (CP) decreases with the solution concentration, but it also leads to lower fluxes [38-40]. The flow rate of both feed and draw solutions is another parameter

affecting the FO process. In general, an increase of the flow rates leads to a low external CP due to better hydraulic conditions and, consequently, to an increase of flux [41, 42].

2.2.3 Draw solutions

The main characteristics of an appropriate solute in the draw solution, i.e. draw solute, are:

- high osmotic efficiency, namely high solubility in water and relatively low molecular weight;
- ideally inert, stable, near neutral pH and non-toxic;
- easily and economically separated to yield fresh water, without being consumed during the process (i.e., minimal reverse draw solute diffusion) [31];
- compatibility with the membrane, i.e. is not harmful for the membrane, chemically and physically [43, 44].

2.2.4 Advantages of the forward osmosis (FO) process

FO has potential benefits mainly associated with the low hydraulic pressure required, the low energy consumption and, thereby, low operation costs. The advantages of FO in water treatment applications are illustrated in Figure 4 [32].

Figure 4: Potential benefits of FO in water treatment.

First, FO requires low energy consumptions if the draw solutes and their regeneration methods are performed economically and technically [45-47]. Membrane fouling is relatively low [48], more reversible [49, 50] and can be minimized by optimizing the hydrodynamics [51]. In addition, a variety of pollutants can be effectively rejected with FO [32].

FO has also the potential to achieve high water flux and high water recovery due to the high osmotic pressure gradient created across the membrane [32]. High water recoveries can reduce the volume of desalination brine, which is a major environmental problem for current desalination plants [52].

Due to the diverse range of potential benefits, FO has been investigated in several other applications [32]. For instance, in the field of food and pharmaceutical processing, FO has the advantage of maintaining the physical properties (e.g. color, taste, aroma and nutrition) of the feed without deteriorating its quality since the feed is not pressurized or heated [53-55]. In medical applications, FO can be applied to release drugs with low oral bioavailability (e.g., poor solubility) in a controlled manner by using osmotic pumps [56, 57].

2.3 Motivation and objectives of the thesis

Membrane technologies have gained some attention because of their interesting inherent features. Common membrane separation processes do not need chemical additives, thermal inputs and spent media regeneration making them more popular over other water treatment technologies [58]. In addition, membranes allow water purification even at ionic levels by rejecting solutes, gases, fluids and particles present in the polluted water [59].

Membranes generally consist of a thin surface layer which provides the required perm-selectivity on the top of a more open and thicker porous support which provides mechanical stability [60]. A large number of polymers can be selected for the fabrication of membranes with very different chemical and physical properties, which will have influence on the respective application [36].

The variety of UF/MF membranes comprise from fully hydrophilic polymers (e.g., cellulose acetate – CA) to fully hydrophobic polymers such as polypropylene (PP), polyethylene (PE) and fluoropolymers (e.g., polytetrafluoroethylene – PTFE). Between these two extremes are the polysulfone (PS)/polyethersulfone (PES) family, polyacrylonitrile (PAN) and polyvinylidene difluoride (PVDF) [60]. The repetitive units for PS and PES polymers are shown in Figures 5 and 6, respectively.

As previously indicated, PS membranes are popular as membrane supports in the water treatment technologies. However, their hydrophobic nature is an disadvantage in this type of applications, which demand appreciable hydrophilicity in order to overcome the production costs [61]. One of the ways for increasing the surface hydrophilicity is to blend the PS polymer with a surface modifier with hydrophilic properties [62-64].

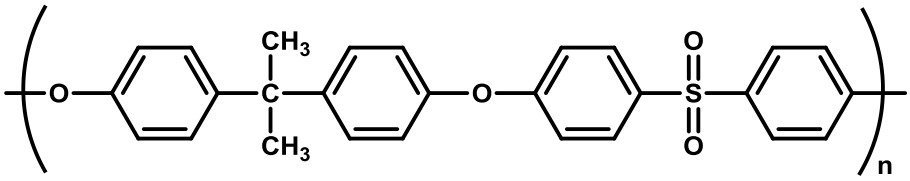

Figure 5: Repetitive unit of the PS polymer.

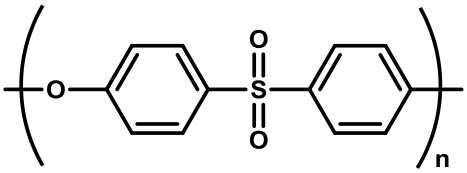

Figure 6: Repetitive unit of the PES polymer.

Titanium dioxide (TiO_2) is a typically semiconductor used as filler in PS blend membranes due to its superhydrophilicity, among other interesting properties [65]. However, TiO_2 may present some compatibility problems with the organic solvents that are used to prepare PS casting solutions, which is an important key to form homogeneous membranes [65].

The use of functionalized carbon materials (e.g., GO and CNTs) in polymeric membranes is currently receiving more attention because unique properties, such as good chemical stability, high surface area [66], mechanical strength [67] and outstanding electron transport [61, 68], can be conferred to the membranes. On the other hand, CNTs and GO are easily functionalized, in this way improving their solubility and facilitating the interaction with a variety of organic solvents and polymers [24-26]. In fact, functionalized multi-walled carbon nanotubes (MWCNTs) and GO have enhanced not only the hydrophilicity [69] but also affected the salt rejection and antifouling properties of carbon PS blend membranes [70-73].

The main objective of this Thesis was to combine functionalized carbon materials with TiO_2 (i.e. carbon-TiO_2 composites) for: (i) enhancing the dispersion of the resulting materials in the solvent and polymer used (e.g., PS) in order to develop homogeneous membranes (i.e. without big holes or strong aggregations); (ii) improving the hydrophilicity of the PS membranes

and (iii) improving the water flux and salt rejection when the membranes are used in filtration processes, including FO.

To reach the main objective, the following specific scientific objectives were defined:

- To prepare PS membranes blended with nanostructured materials, namely CNTs, GO and carbon-TiO_2 composites, studying different synthesis parameters, such as the material loading and the use of a pore former (PVP).
- To develop TFC membranes by using the PS membranes as supports.
- To analyze the morphology, textural and chemical properties of both PS and TFC membranes.
- To study the performance of all membranes in filtration of water and slightly salty water in terms of water flux and salt rejection.
- To evaluate the performance of the TFC membranes in FO, studying FO process variables, such as the different orientation of the active layer and the use of different feed and draw solutions.

Finally, the main technological objective of this Thesis was to design a TFC membrane with high water flux and excellent salt rejection to be applied in desalination driven by FO.

3 Experimental

3.1 Materials

Natural graphite (20 µm, 99.9995%), 1-methyl-2-pyrrolidinone (NMP, 99.5%), polyvinylpyrrolidone (PVP-10K, 10000 g mol^{-1}), 1,3-phenylendiamine (MPD, 99%), 1,3,5-benzenetricarbonyl trichloride (TMC, 98%), ammonium hexafluorotitanate ($(NH_4)_2TiF_6$, 99.99%) and boric acid (H_3BO_3, 99%) were purchased from Sigma-Aldrich. Sodium chloride (NaCl, 99.5%) and n-hexane (C_6H_6, >99%) were supplied from Merck, while magnesium sulfate ($MgSO_4$, 96%) and nitric acid (HNO_3, 65 wt.%) were obtained from Panreac and Fluka, respectively. Polysulfone Udel® P-3500 LCD MB3 was kindly supplied as pellet form by Solvay. Pure polyamide (PA) and polyethersulfone (PES) membranes with 0.22 µm pore size and 25 mm of diameter were purchased from GE Healthcare and Millipore, respectively.

3.1.1 Pristine and functionalized carbon nanotubes

Pristine MWCNTs prepared by CVD were purchased from Nanocyl™ (NC3100 series). MWCNTs presented a carbon purity > 95 wt.%, outer diameter of 9.5 nm, average length of 1.5 µm and an ash content < 5 wt.%.

For the chemical functionalization of MWCNTs, a stainless-steel autoclave (Parr Instruments, USA Mod. 4748) with 125 mL total volume was used. In a typical oxidation experiment, 75 mL of a HNO_3 solution with concentration of 0.30 mol L^{-1} were transferred to a PTFE vessel and 0.2 g of MWCNTs were added. The PTFE vessel was placed into the stainless-steel autoclave, which was sealed and placed in an oven at 473 K for 2 h. After heat treatment, the autoclave was allowed to cool until room temperature. The recovered MWCNTs were washed several times using deionized (DI) water to remove the excess of acid until a neutral pH was achieved in the rising water and then dried overnight at 393 K [22]. The pristine and functionalized MWCNTs will be referred hereafter as MWp and MWf, respectively.

3.1.2 Graphene oxide

Graphite oxide was obtained by the oxidative treatment of commercial graphite following the modified Hummers method as described elsewhere [74]. In a typical procedure, 50 mL of H_2SO_4 was added gradually with stirring to 2 g of graphite and 6 g of potassium permanganate

($KMnO_4$) [75]. The suspension was continuously stirred for 2 h at 308 K. After that, it was cooled in an ice bath and subsequently diluted by deionized water. Then H_2O_2 (30%, w/v) was added in order to reduce residual permanganate to soluble manganese ions, appearing a bright yellow colour in the suspension. The oxidized material was purified with a 10% HCl solution and then the suspension was filtered, washed several times with water until achieve a neutral pH in the resulting water, and dried at 333 K for 24 h to obtain graphite oxide. The resulting material was dispersed in a given volume of water and sonicated in an ultrasound bath (ultrasonic processor UP400S, 24 kHz) for 1 h. The obtained suspension of GO was then used for the synthesis of GO-TiO_2 composites.

3.1.3 Carbon-TiO_2 composites

Carbon-TiO_2 composites were synthesized by using the liquid phase deposition method (LPD) at room temperature and 4 wt.% of carbon material (GO or MWf). The carbon content was selected taking into account previous research works of the group [74], composites prepared with this composition presenting an optimal assembling between TiO_2 and the carbon material. A carbon dispersion in water was previously prepared by sonication in an ultrasound bath for 15 min. In each run, ammonium hexafluorotitanate (IV), $(NH_4)_2TiF_6$ (0.1 mol L^{-1}), and boric acid, H_3BO_3 (0.3 mol L^{-1}), were added to the carbon dispersion heated in an oil bath (333 K for 2 h) under vigorous stirring with the aim to obtain a homogeneous suspension. The precipitate was separated by filtration, washed with water and dried at 373 K under vacuum for 2 h. The obtained solid was treated in a furnace with N_2 flow at 5 K min^{-1} at 473 K with soak time of 3 h [74].

During thermal treatments of carbon-TiO_2 composites, the partial reduction of the carbon material occurs and exclusively anatase TiO_2 particles are formed at such temperatures [74] . The carbon-TiO_2 composites will be denoted as GOT and MWfT, which refers to the type of carbon used, GO and MWf, respectively.

Commercial bare TiO_2 (Degussa P25 from Evonik) with particle size <21 nm was used as reference material and will be referred hereafter as P25.

3.1.4 Polysulfone (PS) membranes

Nanostructured blend PS membranes were prepared by the phase inversion method, studying different synthesis parameters, such as material loading, addition of a pore former

(PVP), as well as the type of material blended. Thus, three nanostructured carbons with different surface chemistry were studied (MWp, MWf and GO) as well as composites prepared with TiO_2 (MWfT and GOT) were compared with P25. In a typical procedure, an appropriate amount of the nanostructured material was first dispersed in 40 mL of NMP by sonication for 10 min until achieving a uniform distribution. Then, PS polymer (12 wt.%) was added to the NMP dispersion under continuous stirring at 343 K for 2h to form a homogeneous casting solution. After that, the PS solution was cool down and kept at room temperature overnight with the aim to remove naturally the air bubbles trapped into the solution.

Later, the degassed solution was casted on a glass dish through spin-coating at 3000 rpm for 1 s and then was immediately immersed into a DI water coagulation bath at room temperature to induce the PS precipitation by a non-solvent/solvent (NMP/water) exchange, forming homogenous membranes. Once the membrane was peeled off from the glass dish, it was transferred to another DI water bath and left for at least 24 h to remove the residual solvent. Finally, the membranes were dried in air at room temperature and stored. For same selected membranes, a 5 wt.% of low molecular PVP was used as pore former and included to the dope solution prior to PS addition. Furthermore, bulk PS membranes (without any amount of material) were also prepared for comparison.

The PS membranes prepared are labelled as: XY/PS-P, where X is the amount of material used (ranging from 0.05 to 0.6 wt.%); P indicates the presence of PVP and Y is the type of material used, i.e. MWp (pristine MWCNTs), MWf (functionalized MWCNTs), MWfT (MWf-TiO_2 composite), GO (graphene oxide), GOT (GO-TiO_2 composite) or P25 (commercial bare TiO_2). More detailed information about the nomenclature and the chemical composition of the PS membranes prepared is shown in Table 1.

3.1.5 Thin film composite (TFC) membranes

All the previous membranes were employed as support (PS substrate) to prepare TFC membranes. The active polyamide layer was formed by interfacial polymerization (IP) on the surface of the PS substrate following a methodology adapted from [76]. In a typical run, the PS substrate was heated at 343 K in a DI water bath for 2 min and the IP process was immediately carried out before it was cooled down at room temperature (Figure 7). For this purpose, an aqueous MPD solution (2% w/v) was poured onto the top surface of the PS substrate for 2 min, ensuring the penetration of the MPD solution into the membrane pores. The excess of the MPD

solution was removed with a rubber roller. Then, a TMC solution (0.1% w/v) in hexane was poured onto the substrate surface for 1 min, the IP process taken place onto membrane surface. After that, the TFC membrane was immersed in pure n-hexane for 1 min in order to remove unreacted monomers from the TFC membrane surface. The TFC membranes were dried at room temperature for 2 min and in an oven at 323 K for 8 min. Finally, the TFC membranes were stored in DI water. The TFC membranes are referred in the text by adding "TFC" to the PS membrane label indicated in Table 1, since the only difference between PS membranes and TFC membranes is that the later has a TFC layer on the top.

Table 1: Nomenclature and chemical composition of the PS membranes.

Name	Material used (M)	Pore former (F)	PS (wt.%)	M (wt.%)	F (wt.%)
PS	-	-	12	-	-
PS-P	-	PVP	12	-	5.0
0.05MWp/PS	MWp	-	12	0.05	-
0.1MWp/PS	MWp	-	12	0.10	-
0.3MWp/PS	MWp	-	12	0.30	-
0.1MWp/PS-P	MWp	PVP	12	0.10	5.0
0.3MWp/PS-P	MWp	PVP	12	0.30	5.0
0.1MWf/PS	MWf	-	12	0.10	-
0.1MWf/PS-P	MWf	PVP	12	0.10	5.0
0.6MWfT/PS-P	MWfT	PVP	12	0.60	5.0
0.1GO/PS	GO	-	12	0.10	-
0.1GO/PS-P	GO	PVP	12	0.30	5.0
0.6GOT/PS-P	GOT	PVP	12	0.60	5.0
0.6P25/PS-P	P25	PVP	12	0.60	5.0

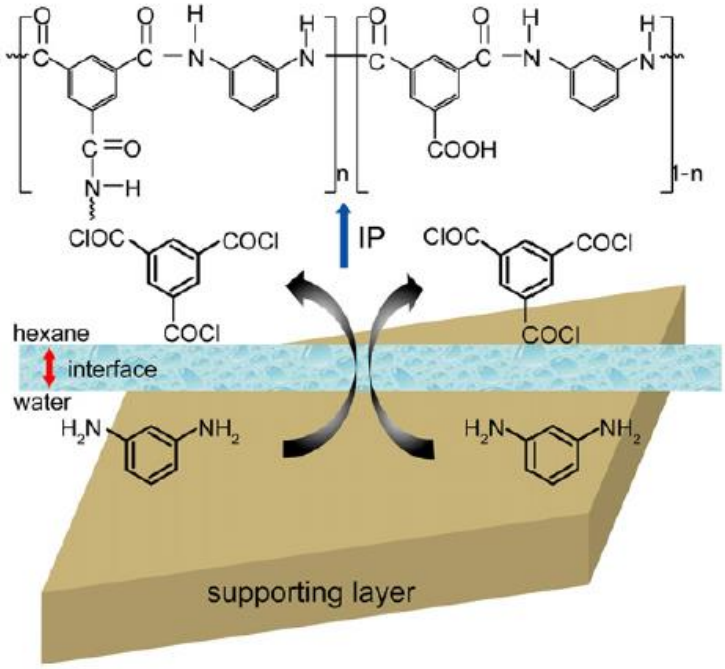

Figure 7: Schematic illustration of the interfacial polymerization (IP) process in TFC membranes**.**

(Figure reprinted with permission from [77]. Copyright 2013, Elsevier.)

3.2 Characterization of the membranes

The morphological analysis and roughness of the membranes were determined by scanning electron microscopy (SEM) using a FEI Quanta 400FEG ESEM/EDAX Genesis X4M instrument. The membranes were frozen and broken by using liquid nitrogen. The microscope was equipped with a special multiple sample holder, in which the broken membranes were vertically positioned to analyze the cross-section of the membranes.

The overall porosity (ε) of the membranes was determined by the gravimetric method. After measuring the dry weight of the membranes, they were immersed in isopropyl alcohol (IPA) overnight to assure the solvent penetration into the membrane pores and then their wet weight was registered. The porosity was calculated by applying eq. 2:

$$\varepsilon\,(\%) = \frac{(m_w - m_d)/\rho_{IPA}}{(m_w - m_d)/\rho_{IPA} + m_d/\rho_p} \times 100 \qquad \textbf{(eq. 2)}$$

where m_w and m_d are the weights of the wet and dry membranes, respectively, and ρ_{IPA} and ρ_p are the IPA (0.786 g cm^{-3}) and polymer (1.240 g cm^{-3}) densities, respectively. Four membranes prepared by the same methodology were used to determine an average value of the porosity, the standard deviation found being lower than ± 1%.

N_2 adsorption-desorption isotherms at 77 K were measured using a Quantachrome NOVA 4200e multi-station apparatus. The apparent surface area (S_{BET}) was determined by applying the Brunauer–Emmett-Teller (BET) equation [78]. The volume of N_2 adsorbed at a relative pressure of 0.95 (V_p) was also obtained from the adsorption isotherms, which corresponds to the sum of the micro- and mesopore volumes according to Gurvitch's rule [79].

The bubble-point method was used to determine the largest pore size of the membranes [80, 81]. In this method, the pressure is slowly increased to one side of the membrane using a compressed gas (nitrogen). When the liquid starts to leave the pores, gas bubbles can be observed on the permeating side of the membrane, and the flow rate becomes non-zero. The gas pressure required to reopen the pores is known as bubble point or pressure. The pore diameter (d_{pore}) can be calculated by eq. 3:

$$d_{pore} = \frac{4\gamma\cos\theta}{P_{bubble}} \qquad \textbf{(eq. 3)}$$

where γ is the surface tension coefficient of the liquid (72 dynes cm^{-1} for isopropanol), θ is the contact angle of the liquid on the pore wall, and P_{bubble} (bar) is the bubble pressure.

The hydrophilicity of the membrane surface was determined by water contact angle measurements using a DataPhysics apparatus (model OCA 15 Plus Germany) that allowed image acquisition and data analysis. The measurements were performed at room temperature, using the sessile drop method of water on dry membranes. Each contact angle was measured for at least 5 different locations on the membranes to get the average value.

The surface chemistry of the carbon materials was characterized by temperature programmed desorption (TPD), as described elsewhere [82, 83]. The point of zero charge (pH_{PZC}) of the nanostructured materials was determined following the methodology published elsewhere [21]. Briefly, 50 mL of NaCl 0.01 M solution was placed in a vessel and the pH was adjusted to a value between 2 and 12 by adding HCl 0.1 M or NaOH 0.1 M, respectively. A 0.15 g sample was added to each vessel and the final pH was measured after 24 h of continuous stirring at room temperature. The pH at which the curve crosses the line $pH_{initial} = pH_{final}$ is taken as the pH_{PZC}.

3.3 Filtration

The performance of the all membranes (i.e. PS membranes and TFC membranes) was evaluated through the determination of the permeate flux of DI water and a slightly salty aqueous solution (1000 ppm of NaCl). Water flux measurements of the membranes were carried out in a stirred filtration cell (Millipore, model 8010). This cell has a total volume of 10 mL, an effective surface area of 4.1 cm^2 and operates at variable pressures and dead-end flows (Figure 8).

All membranes were initially soaked in an aqueous ethanol solution (30:70 v/v) for at least 2 h and then mounted on the filtration unit, which was filled with 10 mL of solution (DI water or salty water). After that, the cell was pressurized and then the permeated volume at a given time was registered under steady flow and 298 K. The water flux (J_w, L h^{-1} m^{-2}) for each membrane was determined by applying the eq. 4 and studied under variable trans-membrane pressures (TMP), ranging from 1.5 to 4.5 bar.

$$J_w = \frac{\Delta V}{A_m \times \Delta t} \qquad \textbf{(eq. 4)}$$

where ΔV is the permeate volume (L), A_m is the effective area of the membranes (m^2), and Δt is the sample time (h).

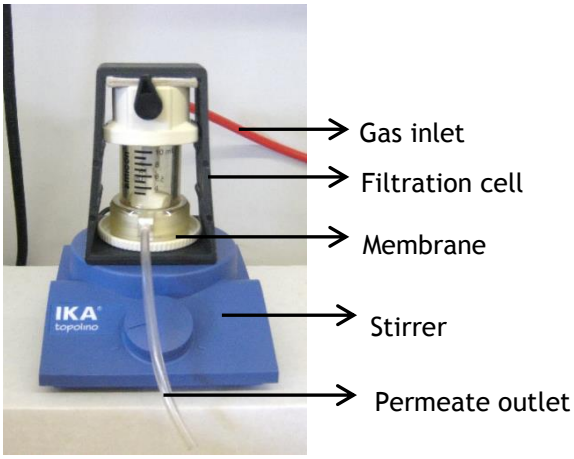

Figure 8: Stirred cell used for the water flux measurements.

For the filtration experiments salty solution, the ionic conductivity was measured in the feed and draw streams by using a conductivity meter (VWR mod.310) and ion chromatography (Metrohm, mod. 881 Compact IC pro) to determine the percentage of salt rejection by applying eq. 5. The concentration of specific cations and anions in the withdrawal samples were also

analyzed with the ion chromatograph equipped with a column of cation and anion exchange (Metrosep C4-250 and Metrosep A Supp 7-250, respectively).

$$\text{Salt rejection } (\%) = \left(1 - \frac{C_p}{C_f}\right) \times 100 \qquad \textbf{(eq. 5)}$$

where C_p is the value of permeate and C_f is the feed concentration.

3.4 Forward osmosis

The TFC membranes presenting the best performances in filtration studies were selected for FO experiments using a home-made built FO unit (Figure 9). This FO prototype basically consists of feed and draw reservoirs placed on weighting scales, a "H-shape" glass FO module and a peristaltic pump. In a typical run, the membrane was placed into the FO module operating in concurrent-flow (effective membrane area of 2 cm^2) at room temperature. Then, 100 mL of DI (0.06 mM NaCl - feed) and salty (0.6 M NaCl - draw) waters were pumped in recirculation mode at similar flow rates (ca. 0.63 L h^{-1}). The osmotic pressure ($\Delta\pi$) difference between the feed and draw solutions was around 15.0 atm (determined from the van't Hoff equation - eq. 1). Ionic conductivity was measured in both feed and draw streams by using a conductivity meter (VWR mod.310) and ion chromatography (Metrohm, mod. 881 Compact IC pro) to determine the percentage of salt rejection (eq. 5). The water flux (J_w, eq. 4) was calculated by measuring the weight change of the feed and draw containers.

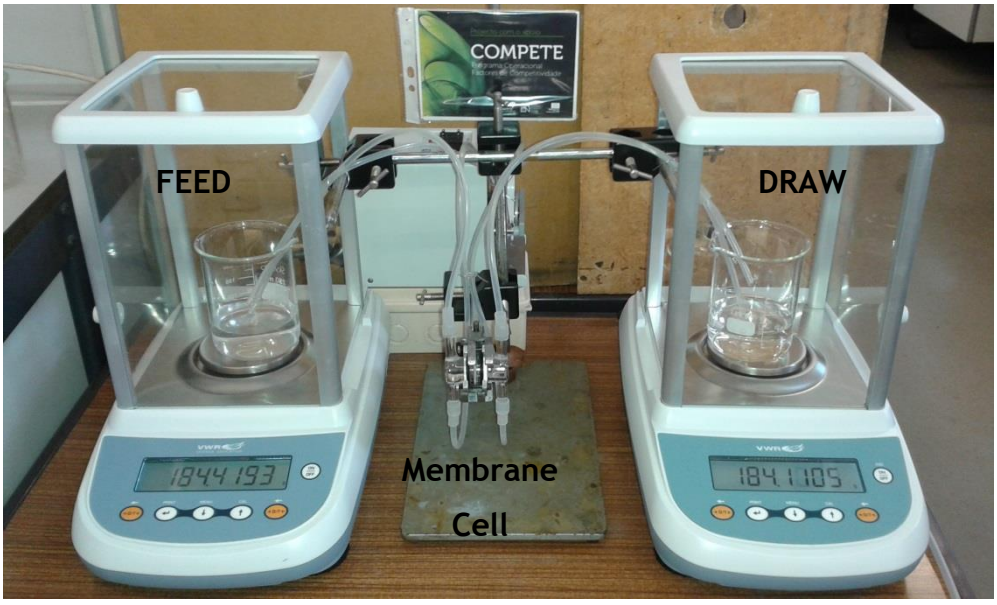

Figure 9: Prototype used in the FO experiments.

In FO experiments, the reverse solute flux (J_s, g m^{-2} h^{-1}) is another important parameter defining the membrane performance which indicates the amount of draw solute across membrane from the draw side to the feed side, and it was determined from the increase of the feed conductivity by using eq. 6 [84]:

$$J_s = \frac{\Delta(C_t \times V_t)}{A \times \Delta t} \qquad \textbf{(eq. 6)}$$

where C_t is the salt concentration (determined with the conductivity meter) and V_t is the volume in the feed stream at a given time (t).

Finally, the TFC membrane with the best performance (0.6GOT/PS-P) was tested by using different feed and draw solutions: (i) DI water and 1.2 M NaCl solution, respectively; and (ii) 0.6M NaCl and 1.25 M magnesium sulfate ($MgSO_4$) solutions, respectively. In general, the experimental conditions were similar to those previously commented, although the osmotic pressure (Δπ) was ca. 30.0 and 15.5 atm for each case.

4 Results and discussion

4.1 Characterization of the nanostructured materials

The morphology of the nanostructured materials before incorporated in the PS membranes was studied by SEM. Figures 10a-d show representative SEM images of MWf, GO, MWfT and GOT, respectively. Figures 10a and c show the different morphology of the carbon materials, MWf and GO, respectively. The MWf material consists of agglomerated carbon nanotubes, while GO clearly shows a structure formed by intercalated GO sheets. The composites presented different morphologies depending on the carbon material used and the accessibility for TiO_2 assembling during the preparation method. In particular, CNTs were observed rolling up the TiO_2 particles in MWfT (Figure 10b), while the TiO_2 particles were uniformly assembled on both sides of GO nanosheets for the GOT composite (Figure 10d).

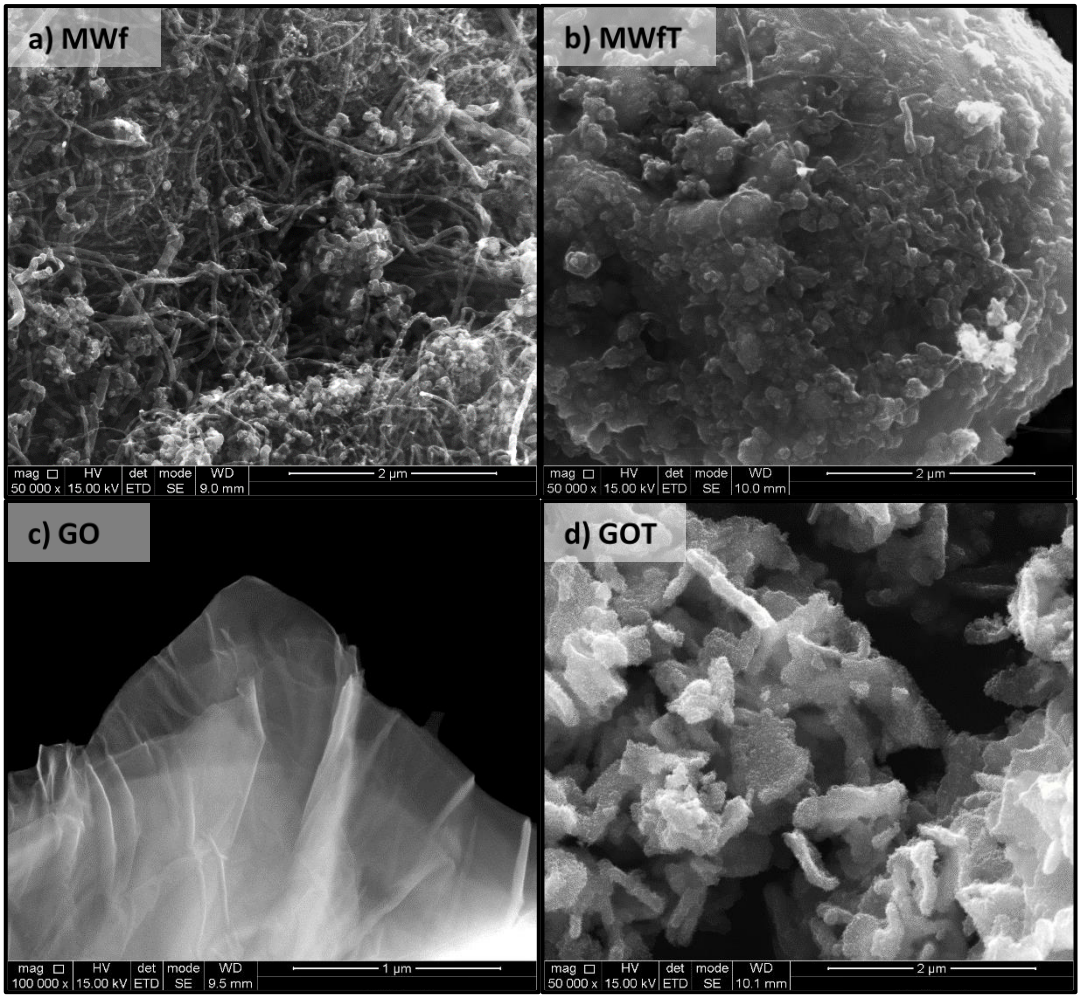

Figure 10: SEM micrographs for a) MWf, b) MWfT, c) GO and d) GOT.

Table 2 summarizes the textural and chemical properties of the nanostructured materials used in this Thesis. The BET surface area (S_{BET}) and the total pore volume (V_p) of the materials were determined, GO presenting the lowest S_{BET} (21 m^2 g^{-1}) and V_p (0.03 cm^3 g^{-1}) [74] while MWf the highest values of S_{BET} (400 m^2 g^{-1}) and V_p (0.65 cm^3 g^{-1}). Both MWfT and GOT presented a higher S_{BET} and V_p than P25. Different trends were observed for the carbon-TiO_2 composites depending on the type of carbon material used. . The lower S_{BET} for the composite prepared with CNT, when compared to GOT, may be due to a larger agglomeration of TiO_2 particles, in the case of MWfT (Figure 10b). In the case of GOT, a significant development of the porosity (i.e., S_{BET} and V_p) was obtained compared to GO.

Table 2: Textural and chemical properties of the nanostructured materials.

Sample	S_{BET} (m^2 g^{-1})	V_p (cm^3 g^{-1})	O_{TPD} (wt.%)	pH_{PZC}
P25	55	0.13	-	6.3
MWf	400	0.65	9.2	4.4
MWfT	86	0.16	-	-
GO	21	0.03	23.6	2.8
GOT	110	0.17	-	3.2

The surface chemistry of the materials was modified by introducing oxygen functional surface groups, leading to acidic properties (Table 2). In general, the presence of oxygen-containing groups improves the interaction between the carbon phase and the TiO_2 particles by the formation of Ti-O-C bonds [85]. The oxygen content (O_{TPD}, Table 2) calculated from the amounts of CO and CO_2 evolved during TPD experiments, was higher for GO than for MWf (23.6 wt.% and 9.2 wt.%, respectively). In this context, the hydrothermal functionalization performed with HNO_3 over MWp was less effective than the method used for GO, the later including stronger oxidants.The high oxygen content detected for GO corresponds to a much larger CO and CO_2 evolution in comparison with MWf during TPD experiments. The low pH_{PZC} determined for GO and GOT indicated a larger acidity compared with the other materials. The surface chemistry of GO should be then responsible not only for its high dispersion in the solution during the preparation of the composites, but also for the good assembly of the TiO_2 particles on GO, as studied by SEM (Figure 10d).

4.2 Characterization of the membranes

The cross-section and surface SEM images for 0.6GOT/PS-P (as example) are shown in Figure 11. The typical asymmetric structure consists of a top porous layer and a fully formed below by macropores (Figures 11a and b). On the contrary, a top dense layer and a porous sub-layer were observed for the neat PS membrane (images not shown). The morphology of the GOT composite (Figure 10d) was not detected onto the surface/layer of 0.6GOT/PS-P (Figure 11c). Thus more SEM analysis are needed in order to confirm how GOT is distributed in the membrane. In general, the differences of morphology were associated with the size and the amount of finger-like pores (Figure 11b), more abundant and larger of size being observed for PS membranes blended with carbon-TiO_2 composites (GOT and MWfT) and functionalized CNTs (MWf). These changes described in the morphology could be due to the increase of the hydrophilicity of the casting solution by the addition of these hydrophilic materials, which increased the permeability of the resulting membrane due to the enhanced phase separation with the material [86].

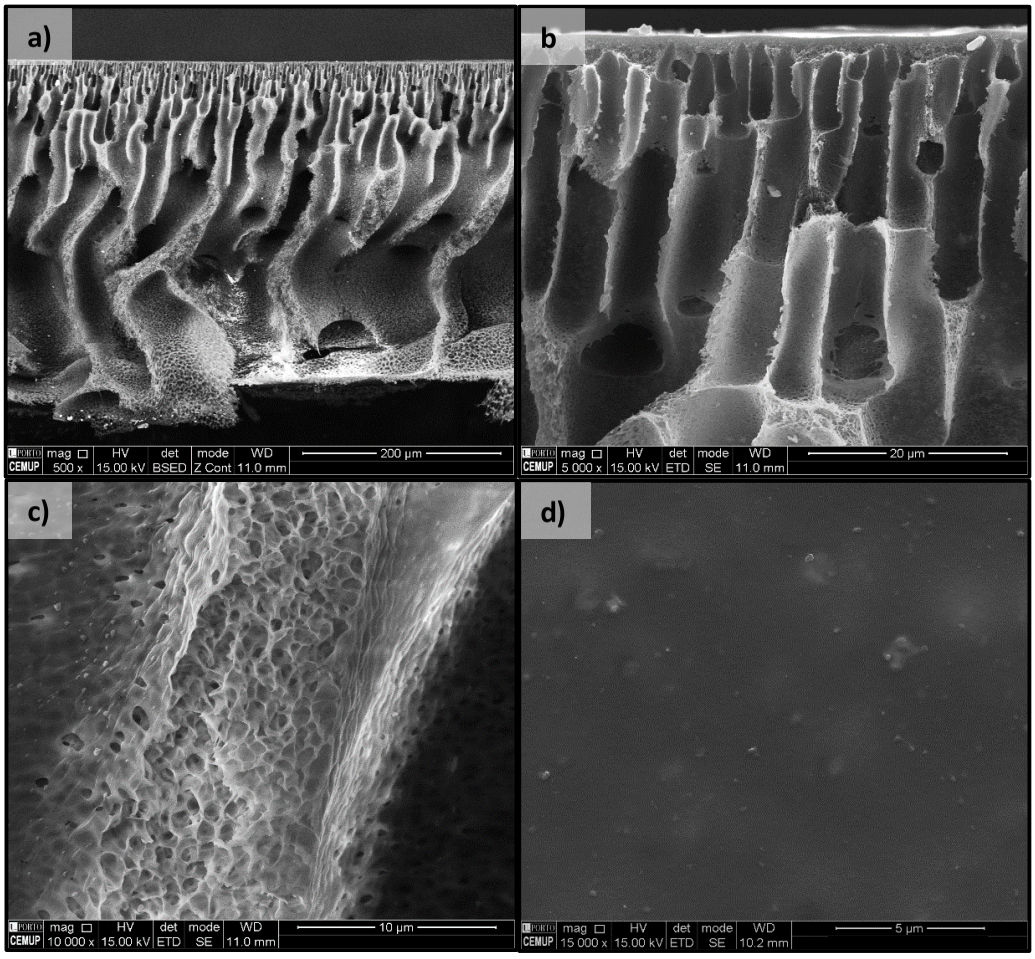

Figure 11: SEM micrographs for the 0.6GOT/PS-P membrane: (a-c) cross section and (d) top images.

The corresponding blend PS membranes did not present an appreciable development of the microporosity and mesoporosity, which is the typical range of porosity determined by physical adsorption of N_2 at 77 K. In this way, the values of S_{BET} and V_p shown in Table 3 for some modified membranes were low and comparable to those obtained for the neat PS membrane (e.g., S_{BET} = 35 m^2 g^{-1} and 38 m^2 g^{-1} for 0.3MWp/PS-P and PS, respectively), which could be indicative of the material immobilization into the membrane structure.

Table 3: S_{BET} and V_p determined for some blended PS membranes.

Sample	S_{BET} (m^2 g^{-1})	V_p (cm^3 g^{-1})
PS	38	0.13
0.05MWp/PS	36	0.13
0.3MWp/PS	38	0.08
0.1MWf/PS-P	21	0.05
0.3MWp/PS-P	35	0.08
0.1GO/PS	32	0.08
0.6GOT/PS-P	24	0.05

The overall porosity and the largest pore size (d_{pore}) were obtained by applying the gravimetric method and bubble point measurements, respectively (Table 4). In general, the PS membranes blended with nanostructured materials presented higher values of porosity (around 82-89%), than those obtained for the neat PS membrane and both commercial PES and PA membranes (84%, 78% and 73%, respectively). The d_{pore} of the membranes seems also to be influenced by the amount and the kind of nanostructured material used, as well as the addition of PVP, larger pore sizes being typically obtained for blend PS membranes in comparison with that of neat PS membrane. For instance, d_{pore} was 2.50, 2.90 and 8.70 µm for PS, 0.1MWp/PS and 0.3MWp/PS, respectively.

On the other hand, changes were produced not only on the physical properties of the membranes but also on the surface hydrophilicity. In this case, the addition of any amount and type of nanostructured material led generally to higher contact angles in comparison with PS, PES and PA. The membranes with lowest contact angles and consequently most hydrophilic,

were those synthetized by using MWf, carbon-TiO_2 composites or P25. This fact could be explained by the hydrophilic properties of the fillers used during the preparation of the membranes.

Table 4: Porosity, contact angle, bubble pressure (P_{bubble}), pore diameter (d_{pore}) and thickness for the PS membranes modified with nanostructured materials.

Name	Porosity (%)	Contact angle (°)	P_{bubble} (bar)	d_{pore} (µm)	Thickness (mm)	Porosity* (%)	Thickness* (mm)
PES	78	68	1.40	0.62	0.170	78	0.171
PA	73	66	0.90	0.96	0.134	77	0.145
PS	84	77	0.35	2.50	0.151	83	0.239
PS-P	88	89	0.15	5.80	0.271	88	-
0.05MWp/PS	84	90	0.30	2.90	0.104	82	0.108
0.1MWp/PS	86	80	0.30	2.90	0.085	83	0.096
0.3MWp/PS	85	87	0.10	8.70	0.164	78	0.099
0.1MWp/PS-P	88	82	0.25	3.50	0.163	84	0.174
0.3MWp/PS-P	82	80	0.20	4.30	0.159	88	0.150
0.1MWf/PS	85	76	0.60	1.50	0.158	81	0.121
0.1MWf/PS-P	89	78	0.20	4.30	0.094	87	0.239
0.6MWfT/PS-P	88	79	0.30	2.90	0.306	88	0.287
0.1GO/PS	85	81	0.60	1.50	0.107	81	0.059
0.1GO/PS-P	90	-	0.25	3.50	0.202	-	-
0.6GOT/PS-P	89	78	0.30	2.90	0.175	87	0.256
0.6P25/PS-P	89	79	0.25	3.50	0.250	88	0.257

* The porosity and the thickness of the corresponding TFC membranes were also included for comparison.

As previously commented, some PS membranes were used as supports of TFC membranes. When the active PA layer was deposited on the PS support, changes were produced on the morphology, textural and chemical properties of the resulting membranes. Thus, the morphology of 0.1MWp/PS-TFC showed as the PA layer was deposited throughout the membrane surface even penetrating into the finger-like pores (Figure 12a) and obtaining a

ridge-valley surface (Figure 12b), which is typical for TFC membranes as a result of the interaction between MPD and TMC during the interfacial polymerization [76]. For TFC membranes, a decrease of the overall porosity (Table 4) and the contact angle (data not shown) were often obtained and compared to the corresponding PS support.

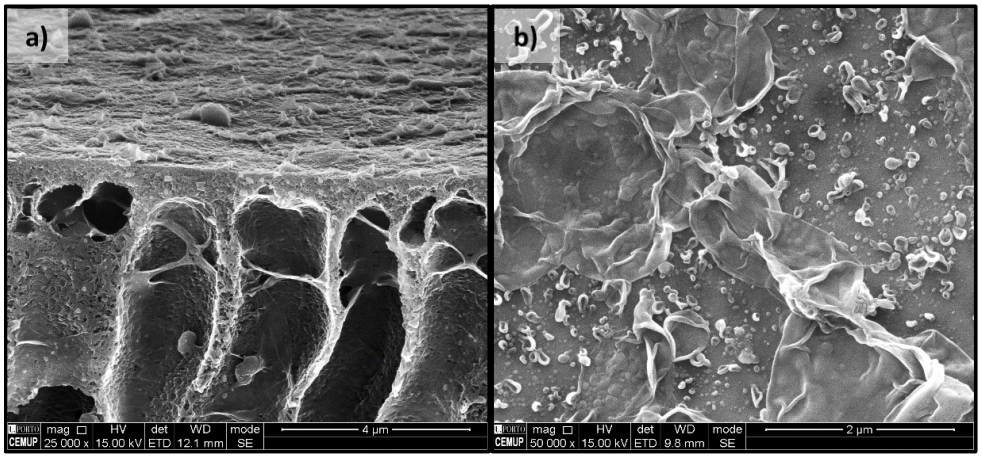

Figure 12: SEM micrographs for the 0.1MWp/PS-TFC membrane: (a) cross section and (b) top images.

4.3 Filtration by using polysulfone PS membranes

The permeation performance of the membranes was evaluated by flux measurements of DI water and then, 1000 ppm NaCl solution. The water flux and salt rejection were also determined by varying the trans-membrane pressure (TMP), and the membrane properties were correlated with the permeation results.

4.3.1 Measurement of the water flux in filtration of DI water

The performance of the prepared PS membranes was analyzed in filtration of DI water and the water flux was determined. The first test was to study the variation of the water flux with TMP. The results are presented in Figures 13a-b for membranes modified with nanostructured materials and TFC membranes, respectively.

As can be observed, an increase in TMP implied a better flow of water through the membrane regardless the membrane composition, the highest permeation being obtained at 4.5 bar of pressure. In general, high pressures in filtration cause membrane compaction leading to high flux values [87, 88]. However, high TMP may produce irreversible changes to the macro-void structure of the membrane, resulting in decreased pore volumes and non-recoverable lost in hydraulic permeability [88].

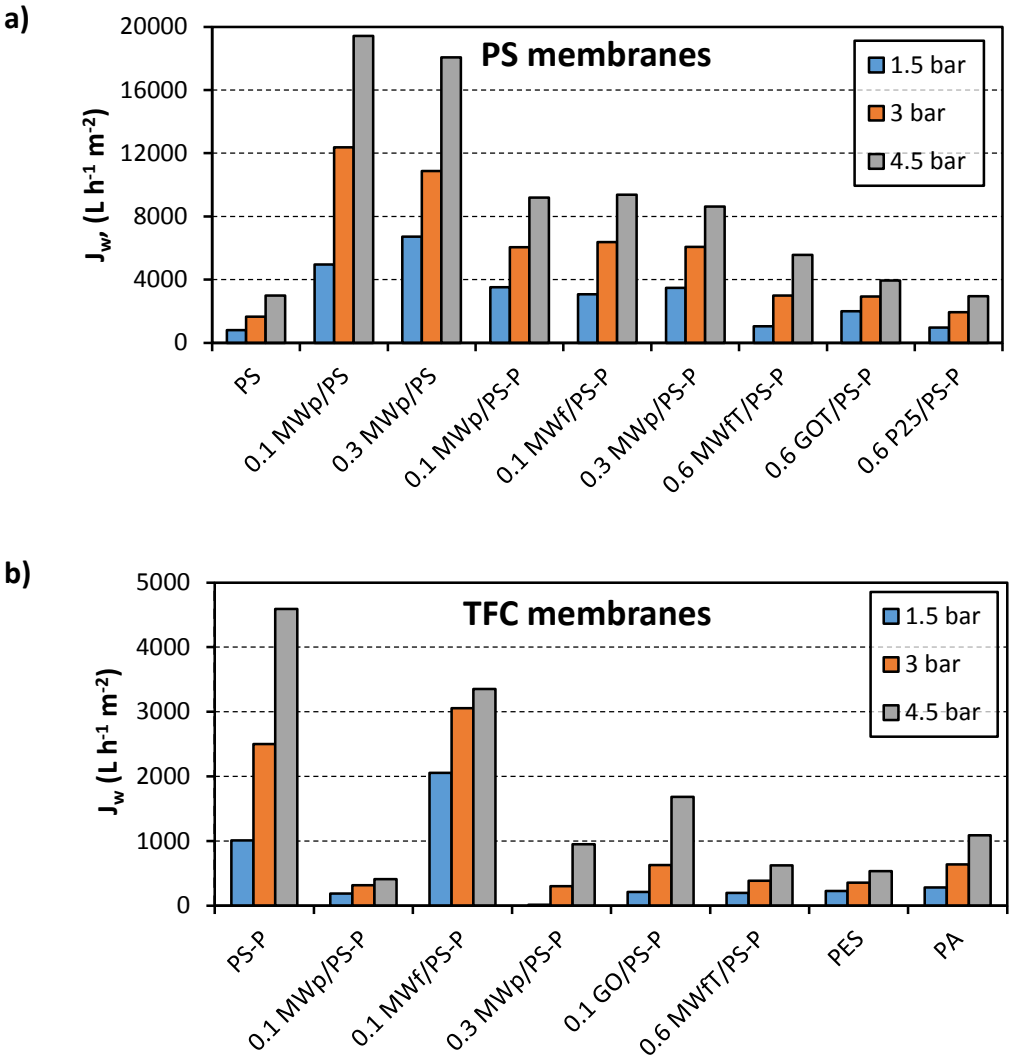

Figure 13: Water flux obtained in filtration at different TMP. Performance for (a) PS membranes blended with nanostructured materials and (b) TFC membranes.

The PS membranes blended with 0.1 wt.% of MWp (0.1MWp/PS) and without PVP additive showed the best performance in filtration; the water flux is significantly higher than that observed for the neat PS membrane. The flux at 4.5 bar determined for 0.1MWp/PS (19429 L h^{-1} m^{-2}), was also higher than that obtained for GO or TiO_2 blended PS membranes. Furthermore, membranes modified with the nanostructured materials are more resistant to compaction that the corresponding neat polymer homologues [89-91].

On the other hand, the neat PS membrane (PS) presented a higher thickness compared to PS membranes blended with MWp, which should contribute for the low water flux observed, since high thickness induces usually to large ICP effect.

For the membranes with the same amount of carbon-TiO_2 (0.6 wt.%) and PVP additive (Figure 13a), the highest flux was obtained for 0.6MWfT/PS-P. Thus, the combination between

MWf and TiO_2 seems to give membranes with high flux values (5569 L h^{-1} m^{-2} at 4.5 bar). Therefore, MWf seems to be more efficient that GO to improve the water permeation of PS membranes modified with carbon-TiO_2 composites.

Apparently, the use of PVP in the PS membranes did not allow to enhance the water flux compared to other membranes without this additive in the composition (Figure 13a).

On the other hand, TFC membranes prepared by using the PS membranes as supports, exhibited a decrease of the flow compared to the original PS membranes (Figure 13b), which may be due to the lower porosities determined for TFC (Table 4) [76] . In spite of low permeation, TFC membranes prepared on 0.1MWf/PS-P and 0.6MWfT/PS-P showed better results than those synthetized on commercial membranes (PES or PA).

4.3.2 Measurement of the water flux in filtration of slightly salty water

After water flux measurement, the membranes were tested in filtration with consecutive cycles: first DI water, then slightly salty solution (1000 ppm NaCl) and finally DI water again. The results are presented in Figures 14a and b for membranes modified with nanostructured materials and TFC membranes, respectively.

In general, a decline of the flux was always observed when salty water was used in the second cycle and the flux was not recovered when DI water was again used in the third cycle. The slight decrease of the flow over time could be due to the concentration polarization, adsorption and pore blocking (fouling) [66]. Under our experimental conditions, the membrane was only pre-treated at the beginning of the first cycle and, thereby, the membrane was not fully regenerated after each filtration cycle, as well as its ability to permeate was not restored.

The PS membranes modified with CNTs and without PVP presented better water flux than the neat PS membrane and an optimal amount of MWp added seems to be reached with 0.1 wt.% of MWp. In fact, 0.1MWp/PS is the most efficient membrane in filtration even for slightly salty water (Figure 14a). This CNTs blend PS-P membrane has a better performance than PS-P. In addition, the 0.1MWp/PS-P membrane prepared with MWp had better performance than that prepared with GO (i.e., 0.1GO/PS-P). Therefore, the use of CNTs as fillers seems to improve the water permeability of PS membranes in the filtration process, as also reported for the case of hollow fibers [92].

In the case of PS membranes blended with carbon-TiO_2 materials, the water permeation varied in the order: MWfT > GO > P25. Therefore, the presence of a carbon phase improved the

performance of the membranes compared with that prepared with P25 which is a material more hydrophilic than MWf and GO and it is commonly used for the preparation of composite membranes [93, 94].

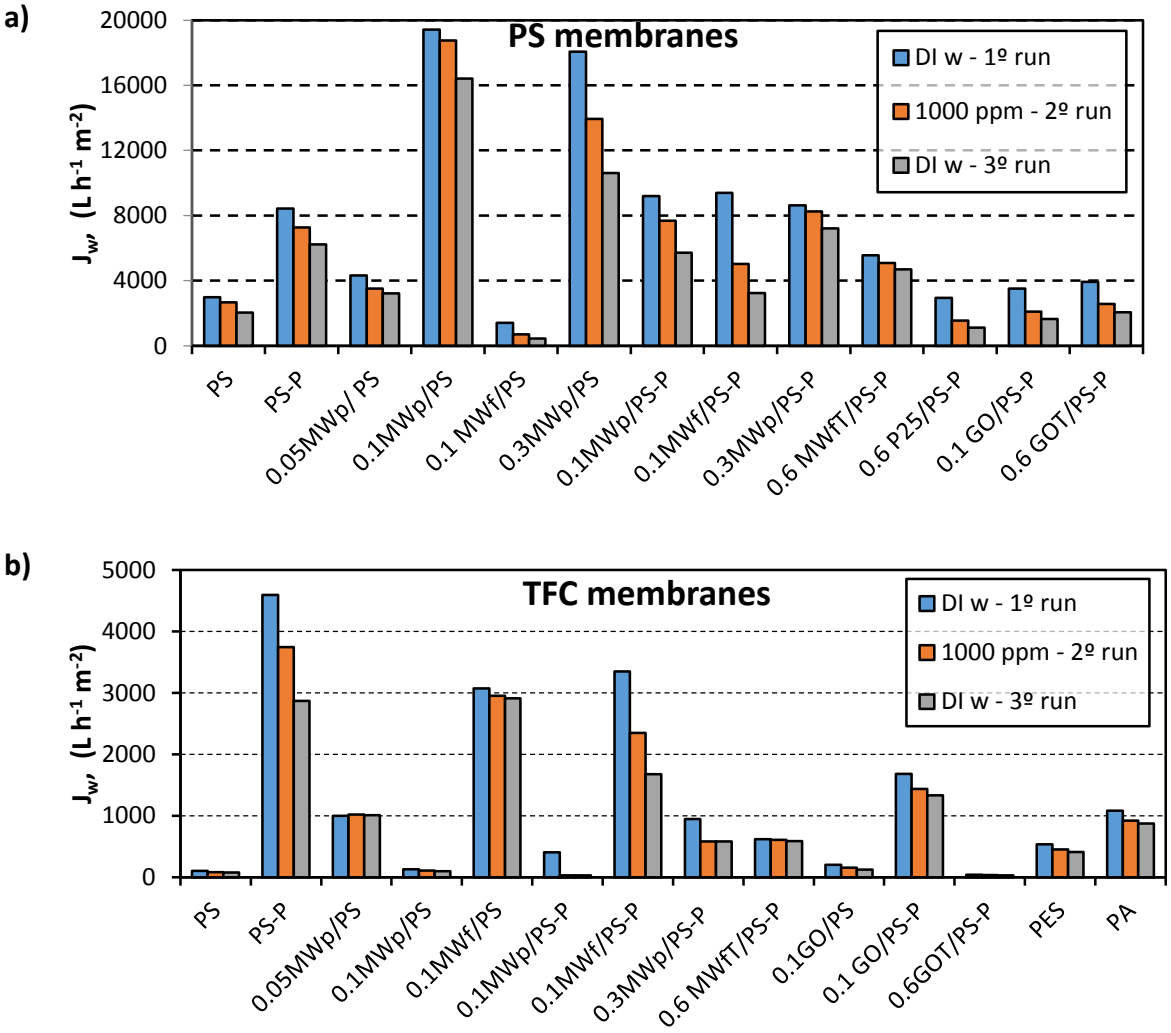

Figure 14: Water flux obtained in filtration at 4.5 bar of different solutions (DI water, 1000 ppm NaCl and DI water). Performance for (a) PS membranes blended with nanostructured materials and (b) TFC membranes.

For TFC membranes the water flux was significantly lower than those obtained by PS membranes blended with nanostructured materials (Figure 14b). The PS/P membrane seems to be more efficient that the others, but this membrane is not so stable as 0.1MWf/PS. In addition, the TFC membranes with functionalized carbon materials (MWf and GO) presented a higher water flux, than that obtained for TFC membranes prepared with commercial supports (PES and PA). Overall, the 0.1MWp/PS membrane was the most efficient regarding water flux and also presents a good stability.

4.3.3 Salt rejection in filtration of slightly salty water

The salt rejection (Na^+ cation and Cl^- anion) of the membranes tested with salty water as feed solution is shown in Figures 15a and b for membranes modified with nanostructured materials and TFC membranes, respectively. In general, all membranes tested presented certain salt rejection, but some differences were found depending on the ion removed and the membrane morphology [95]. In addition, the relationship between the permeate flux and salt rejection is another important factor to take into account. Although there is no an explicit correlation between these two parameters for each membrane, the salt rejection generally decreases with increasing flow since a larger flow is associated with membranes of larger pores, which promote the passage of water and also ions, such as Na^+ and Cl^-.

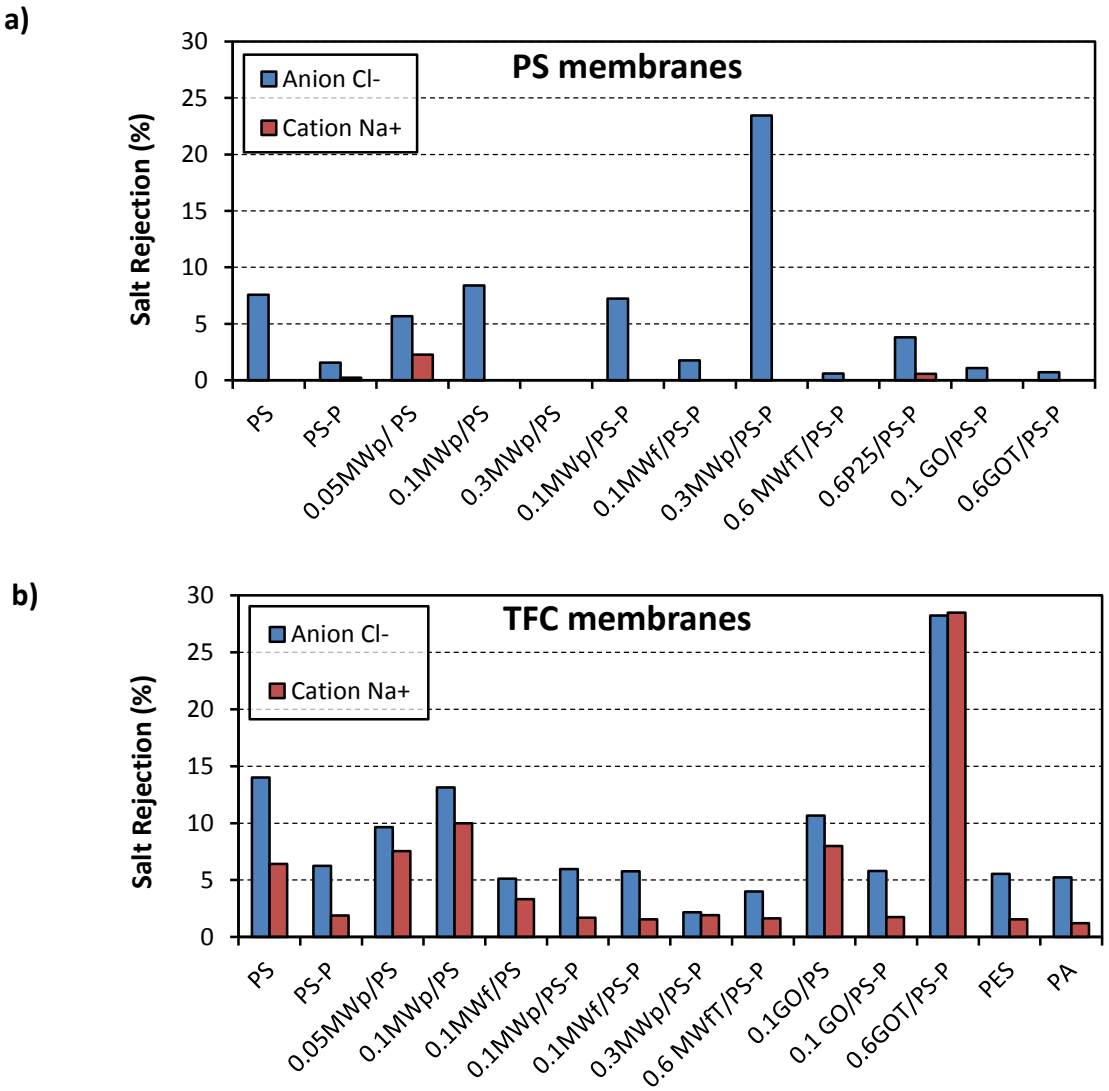

Figure 15: Salt rejection obtained in filtration at 4.5 bar of a 1000 ppm NaCl solution. Performance for (a) PS membranes blended with nanostructured materials and (b) TFC membranes.

Two main conclusions can be addressed from the results shown in Figures 15a and b: (i) TFC membranes have better performance for salt rejection than the asymmetric membranes without a PA active layer [96] and (ii) the removal of Cl^- is higher than for Na^+. This fact can be justified by the low ion size of Na^+ compared to Cl^- (steric effect) or by the electrostatic interactions between the negative charges of Cl^- and the membrane surface [95].

TFC membranes prepared on commercial supports (PES and PA) presented low salt rejection values (ca. 5% for Cl^-), twice less than those obtained with the best membrane in filtration (0.1MWp/PS), i.e. Cl^- removal around 9%. The other membranes presented relatively low salt rejection values taken into account the water flux previously observed (Figure 14b).

The filtration process is not the most adequate method for water desalination, at least with membranes with the range of pores fabricated in the present work. Membranes with pore sizes below 2 nm have showed good results in desalination driven for RO, although they also present some inconveniences. In this context, the TFC membranes presenting higher salt rejection more tested in the FO process.

4.4 Forward osmosis by using thin film composite (TFC) membranes

As mentioned above, the driving force in FO is the osmotic pressure difference between the feed and draw solutions and the FO process can operate in two different modes by changing the orientation of the membrane active layer, i.e. active layer faced to the draw solution (ALDS) or active layer faced to the feed solution (ALFS) [97].

The performance of the membranes in FO is governed by both water flux and solute retention. Thus, selected TFC membranes were tested in FO by using the feed/draw solutions as follows: (i) DI water (0.06 mM NaCl)/0.6 M NaCl solution (C_{NaCl} = 35 g L^{-1}); (ii) DI water/1.20 M NaCl solution (C_{NaCl} = 70 g L^{-1}); and (iii) 0.6 M NaCl/1.25 M $MgSO_4$ solution (C_{MgSO_4} = 150 g L^{-1}).

4.4.1 Performance of TFC membranes by using 0.6 M NaCl as draw solution

The TFC membranes were firstly tested in ALDS configuration and the results are shown in Figure 16. In general, the water flux quickly increased during the first 30 min, and then remained relatively similar until 180 min. This fact suggests that the non-linear increase in flow over time can be attributed to the presence of fouling or ICP [12].

The most efficient TFC membrane was that prepared on 0.1MWp/PS-P and then on 0.3MWp/PS-P (Figure 16a), which also presented high water fluxes in filtration of salty water

(Figure 14a). These membranes presented higher water permeation than that prepared with only PS. The other TFC membranes prepared with CNTs presented low water flux values, which could be due to their moderate hydrophilicity, which would affect their hydraulic resistance and, consequently, their water permeability [98].

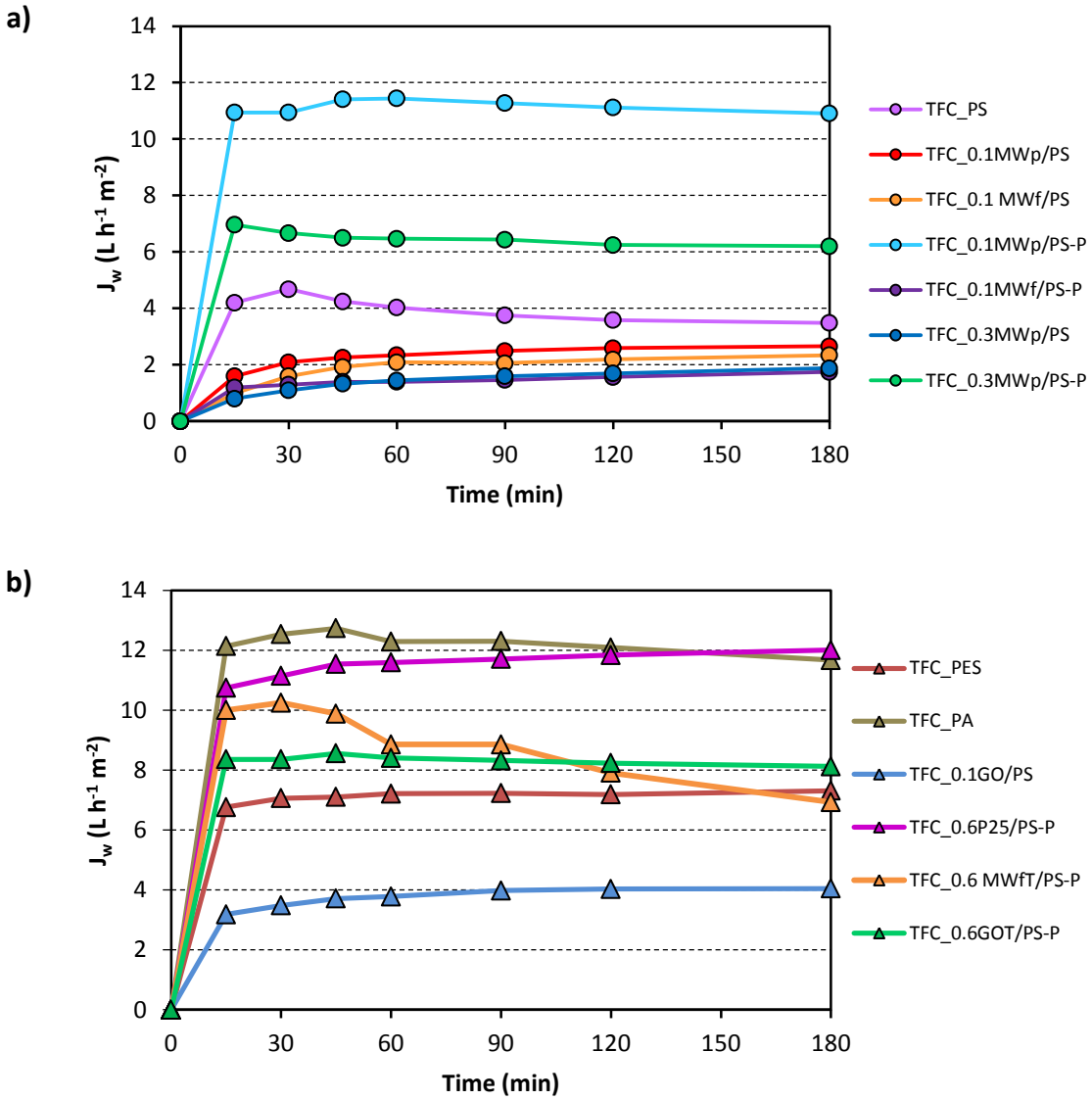

Figure 16: Water flux obtained in FO with ALDS configuration for TFC membranes prepared on PS membranes blended with (a) CNTs and (b) other nanostructured materials.

The use of PVP additive in the PS membranes seems also to influence the performance of the TFC membranes, since 0.3MWp/PS-P and 0.1MWp/PS-P presented higher water flux than their homologues without PVP (Figure 16a).

The TFC membranes without nanostructured materials, such as PS and commercial membranes (i.e. PES and PA), were also tested in FO process. The TFC_PA membrane is the best

performing membrane in ALDS mode (water flow around 12 L h^{-1} m^{-2}). Moreover, the PES membrane has significantly lower values. Table 4 shows that the PES membrane has much lower pore diameter than PA, justifying its lower water flux in FO. The neat PS membrane has also a very low flux in the process, probably as a result of its larger thickness in comparison with the other membranes (Table 4).

One of the most efficient TFC membranes was 0.6P25/PS-P (Figure 16b). Therefore, the hydrophilicity of the PS substrate was significantly improved with the addition of hydrophilic TiO_2 nanoparticles into the dope solution, as previously reported for the contact angle in Table 4. In addition, the water flux obtained for the PS substrate with TiO_2 enhanced the TFC membrane performance, minimizing the transport resistance against water permeation. Thus, all TFC membranes prepared on the TiO_2/PS substrate exhibited much higher water permeability than those prepared with carbon materials, except for TFC membrane 0.1MWp/PS-P.

The quick deactivation observed for 0.6MWfT/PS-P_TFC could be due to the apparition of ICP and, consequently, to the reduction of the effective osmotic pressure. The structure of a membrane may have influence on the resistance to solute diffusion in the porous support. The diffusion coefficient of the draw solute is fixed, leaving only the structural parameter of membranes as a means to reduce ICP. This structural parameter has units of length and can be thought as the characteristic distance a solute particle must travel to reach the active layer of the membrane from the bulk draw solution. FO membranes with thinner, more porous and less tortuous supports will have smaller values of this parameter and produce higher water fluxes [99]. 0.6MWfT/PS-P was the thicker membrane and probably could be more influenced by ICP.

The TFC membranes were again tested in FO under the same experimental conditions but in ALFS configuration to study the effect of the membrane orientation and the results are shown in Figure 17. In general, all TFC membranes presented higher water flux when the active layer of the membrane was facing the draw solution (ALDS orientation), presenting a steady water flux after 15 min. For instance, PA_TFC presented a water flux around 12 L h^{-1} m^{-2} in ALDS orientation, while the water flux decreased until 7 L h^{-1} m^{-2} (42%) in ALFS orientation. However, the opposite effect was observed for 0.6GOT/PS-P_TFC, i.e. the water flux was 8.2 L h^{-1} m^{-2} in ALDS orientation and increased almost twice times until 12.1 L h^{-1} m^{-2} in ALFS orientation.

Most of the studies reported a higher water flux in ALDS mode compared to ALFS mode due to the less effective ICP, since the dense active layer faces the concentrated draw solution and avoids the solute pass through the membrane. In ALDS mode, the hydrophilic and highly

porous substrate faces the feed solution (less concentrated than draw solution), and water flows through the hydrophilic porous substrate with low resistance. Therefore, water flux in ALDS mode should be higher than that in ALFS mode [84].

The results obtained for all membranes are in agreement with this theory with exception of those obtained with 0.6GOT/PS-P_TFC, where an increase of flux and a higher resistance to fouling seems to occur in ALFS mode. So, the ALDS orientation of TFC membranes was generally more vulnerable to fouling, especially for non-commercial membranes, which means that there is a decrease in the performance of these membranes when placed in this orientation. The typical roughness property of TFC materials and other complex mechanisms associated with the multi-components mixed could also have played a role in membrane fouling for both orientations [37].

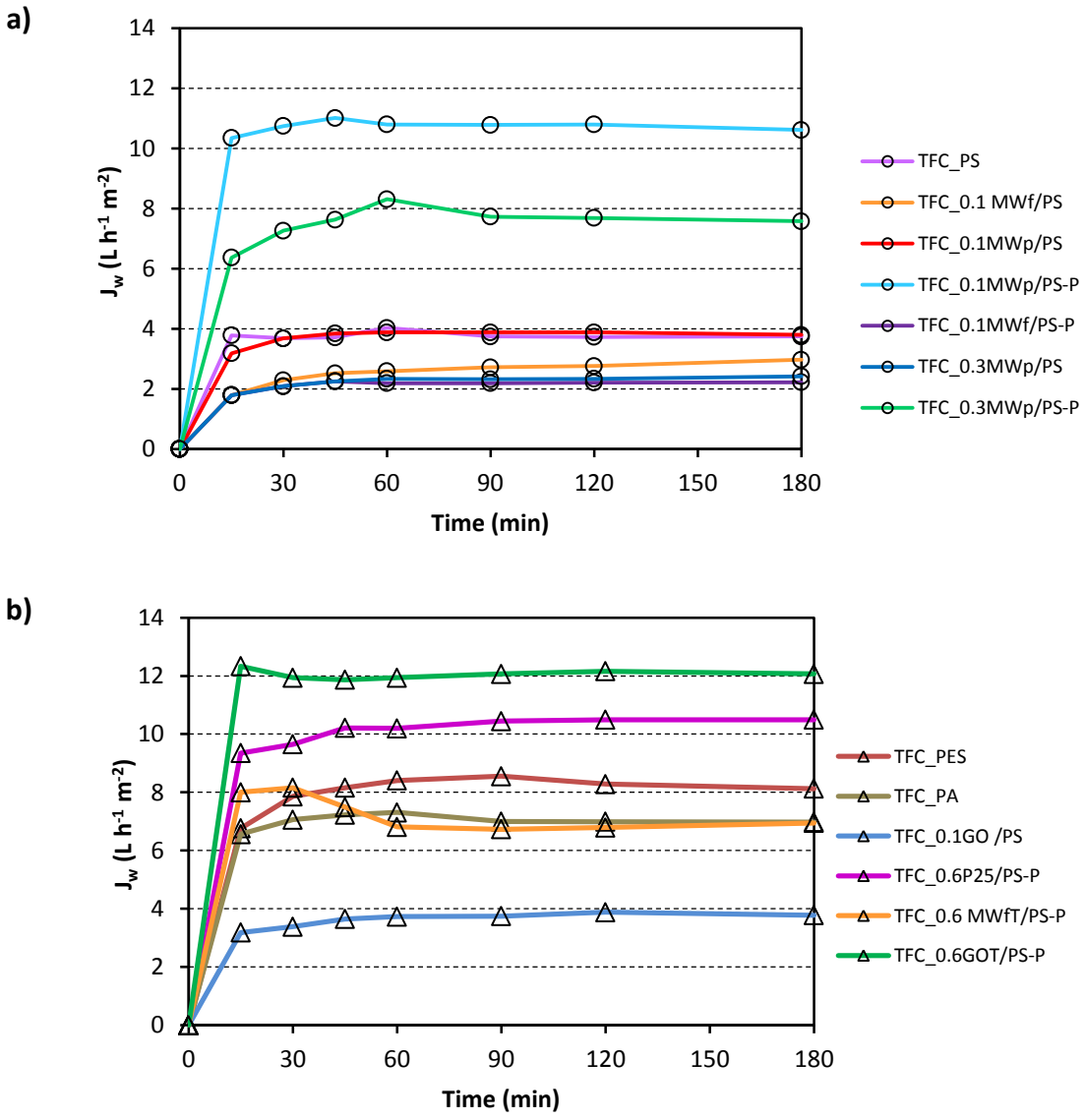

Figure 17: Water flux obtained in FO with ALFS configuration for TFC membranes prepared on PS membranes blended with (a) CNTs and (b) others nanostructured materials.

The performance of TFC membranes in both orientations was also evaluated in terms of salt rejection and reverse solute flux (Figure 18), which is the amount of draw solute (NaCl) that passes through the membrane from the draw solution to the feed solution. In general, all membranes presented moderate reverse solute flux values, although the salt rejection was above 98%. The TFC membranes with higher water flux were those prepared on 0.1MWf/PS-P, PA, 0.6MWfT/PS-P, 0.6P25/PS-P and 0.6GOT/PS-P and on the commercial PA (Figures 16 and 17), while the higher value of reverse solute flux (g h^{-1} m^{-2}) obtained for these membranes decreased as follows: PA (102) > 0.6GOT/PS-P (75) > 0.1MWf/PS-P (50) > 0.6P25/PS-P (43) > 0.6MWfT/PS-P (25). Thus membranes modified with TiO_2 and carbon-TiO_2 particles are more resistant to the passage of the draw solute.

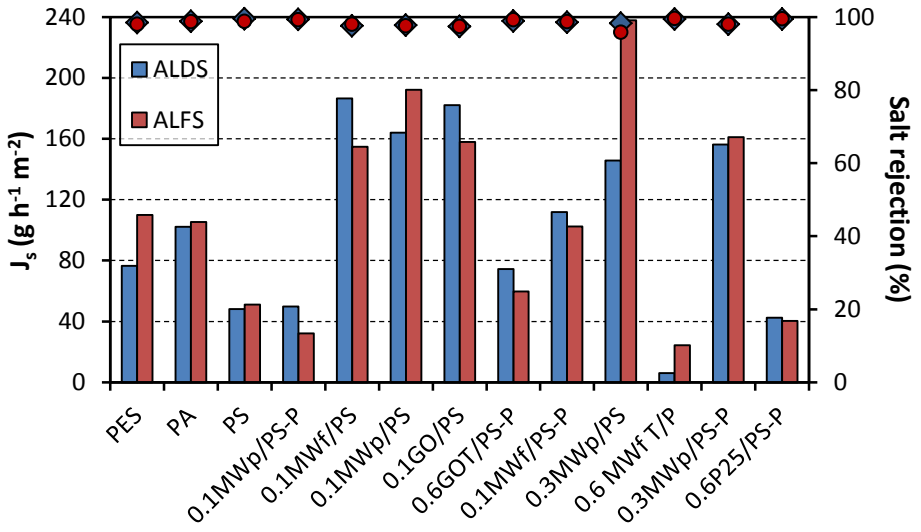

Figure 18: Reverse solute flux (bars) and salt rejection (symbols) (%) obtained in FO for ALDS and ALFS configurations.

Based on the results of water flux (Figures 16 and 17) and reverse solute flux (Figure 18), a correlation was plotted in order to select the most active membrane in FO when using 0.6 M NaCl solution as draw (Figure 19). Therefore, it can be concluded that TFC membranes prepared on PS-P membranes modified with 0.6 wt.% of P25 or GOT, and 0.1 wt.% MWp were the best three performing FO membranes, i.e. with high water flux and low solute flux.

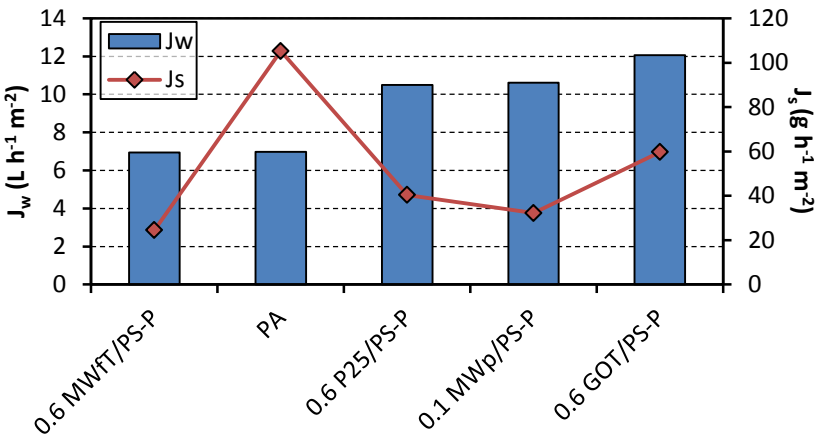

Figure 19: Water flux (J_w) and reverse solute flux (J_s) of selected TFC membranes.

4.4.2 Performance of TFC membranes by using 1.2 M NaCl as draw solution

Figure 20 shows the water and draw reverse fluxes as a function of the draw solution concentration maintaining DI water as feed solution for 0.6GOT/PS-P_TFC. As result of the increase of the osmotic pressure difference over the membrane, the water flux enhanced with the draw solution concentration for ALDS orientation.

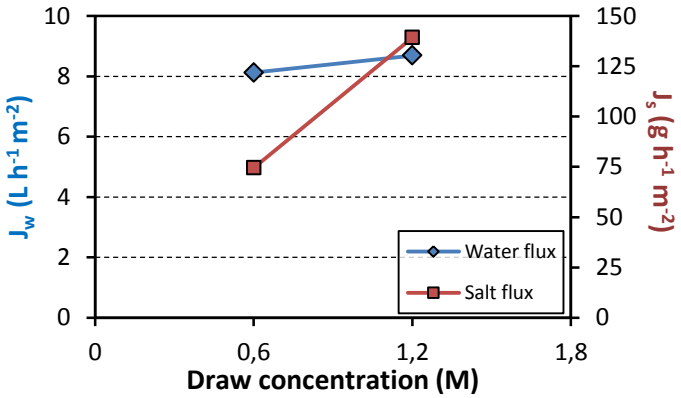

Figure 20: Influence of the draw solution concentration on the water flux and reverse solute flux for the TFC membrane prepared on 0.6GOT/PS-P and using the ALDS orientation

The reverse salt flux was found to increase with the draw solution concentration due to the a larger concentration of salt on the active layer [100].

4.4.3 Performance of TFC membranes by using 1.25 M $MgSO_4$ as draw solution

Water desalination of a solution similar to seawater salt concentration was studied by FO using $MgSO_4$ as draw solute. One of the best membranes in terms of salt rejection and water flux (0.6GOT/PS-P_TFC) was first tested with DI water and 0.6 M NaCl as feed and draw solutions, respectively. After that, the performance of this membrane was assessed but using 0.6 M NaCl and 1.25 M $MgSO_4$, as feed and draw solutions, respectively.

A decrease of the water flux was observed regardless the membrane orientation when $MgSO_4$ was used as draw (Figure 21). This lower performance of the TFC membrane compared to that using DI water and 0.6 M NaCl, respectively as feed and draw solutions, could be due to a larger accumulation of salts in both draw and feed sides and also to the different diffusivity of the electrolytes into the porous structure of the membrane. In general, the diffusion coefficients for bivalent electrolytes ($MgSO_4$) are considerably lower than those for monovalent electrolytes (NaCl), lower water fluxes being obtained for bivalent draw solutions [101].

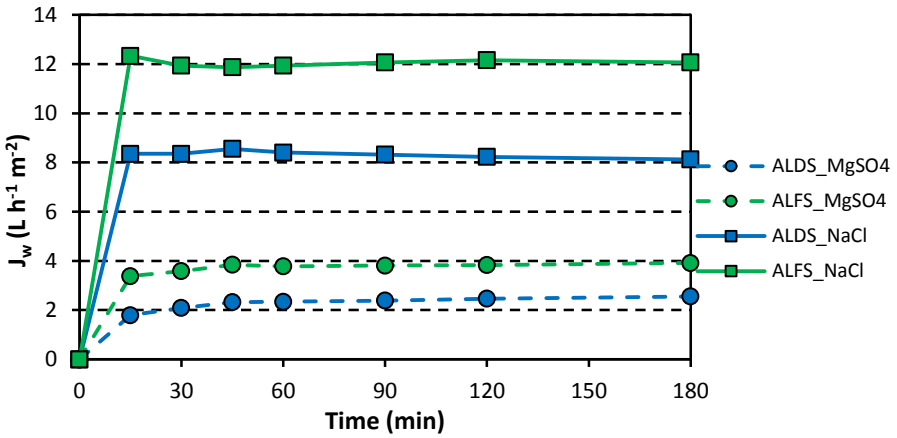

Figure 21: Water flux for 0.6GOT/PS-P_TFC obtained in FO with different draw solutions (NaCl or $MgSO_4$) and membrane orientations (ALDS or ALFS).

On the other, the change of draw solution had not a large impact on the salt rejection or reverse solute flux of 0.6GOT/PS-P_TFC (Table 5). In fact, the reverse solute flux for $MgSO_4$ as draw solution was lower than that for NaCl in ALDS orientation, where the layer active faces the draw solution and avoids the solute transport. This higher rejection could be due to steric or electrostatic interactions because divalent anions are larger and less likely to move through the membrane [100].

Table 5: Influence of the draw solution and the membrane orientation on the performance of 0.6GOT/PS-P_TFC in FO at 180 min.

Feed side	Draw side	Configuration	Water flux (L h^{-1} m^{-2})	Reverse solute flux (g h^{-1} m^{-2})	Draw rejection (%)
DI water	0.6 M NaCl	ALDS	8.1	75	99
DI water	0.6 M NaCl	ALFS	12.1	60	99
0.6 M NaCl	1.25 M $MgSO_4$	ALDS	2.6	62	100
0.6 M NaCl	1.25 M $MgSO_4$	ALFS	3.9	70	100

In spite of the magnesium sulfate lower osmotic pressure compared to sodium chloride, its use in FO as draw solute is very useful in terms of product water recovery. Since magnesium sulfate is highly soluble in water and can be recovered from the diluted draw solution by a precipitation reaction with barium sulfate [102]. Therefore, the next step in the FO process will be to recover the water from diluted draw solution in order to produce fresh water by the FO process.

5 Conclusions

PS membranes blended with CNTs, GO and carbon-TiO_2 composites were prepared by the phase inversion method, studying different synthesis parameters, such as material loading and addition of a pore former, PVP. In general, PS membranes blended with nanostructured materials presented higher porosity and contact angle than those obtained for the neat PS membrane. The pore size (d_{pore}) of the membranes was also influenced by the amount and the type of nanostructured material used, as well as by the addition of PVP; pores with larger size were obtained for blend PS membranes in comparison with those of neat PS membrane.

TFC membranes were prepared by using the PS membranes as supports though interfacial polymerization. The resulting membranes presented a ridge-valley surface and a decrease of the porosity and the contact angle compared to the corresponding PS support.

Both PS and TFC membranes were tested in filtration of DI water and slightly salty water, a linear relationship being found between both trans-membrane pressure (TMP) and water flux. The PS membrane with the best performance in filtration was 0.1MWp/PS. However, the salt rejection of the PS membranes was near 8%. TFC membranes presented lower water flux but higher salt rejection compared to the corresponding PS supports, 0.1MWf/PS being the membrane with the highest water flux and salt rejection.

TFC membranes were tested in FO with DI water and 0.6 M NaCl, as feed and draw solutions, respectively, presenting generally better performance in ALDS configuration than ALFS. The most active TFC membrane in FO (i.e., highest water flux and lowest solute reverse flux) was that prepared on a PS membrane with 0.6 wt.% of GOT (0.6GOT/PS-P_TFC). This membrane was also tested with 1.2 M NaCl draw solution (higher osmotic pressure), an increase of both water flux and solute reverse flux with the concentration of draw solution being observed. Finally, 0.6GOT/PS-P_TFC was tested in FO by using 0.6 M NaCl and 1.25 M $MgSO_4$, as feed and draw solutions, a low water flux and solute flux being obtained.

6 Evaluation of the work done and future work

6.1 Final appreciation of the work done

The development of this project during my Master's Thesis allowed me to understand and learn how to work in a R&D group. This project is giving its first steps, and so a lot of work still needs to be done. In particular, the best combination of different synthesis parameters to design a highly effective membrane in desalination processes, combining reduced energy expenditures to higher performance. The research in the field of nanostructured materials for desalination has not yet reached its maximum peak and needs to be developed conveniently.

In my opinion, the LCM laboratory is provided with very good facilities in this area of research, which enabled the work to be performed with favourable conditions. Although the time to produce all the work expressed in the thesis was very short, there was a proper management of deadlines that allowed it to be possible to present the final result at the right time.

6.2 Future work

The secret to design a membrane that is viable in a desalination process involves improving its structure and composition. Modifications made to the membrane are also fundamental to achieve perfection.

Concerning the thin-film composite membranes, further improvements are needed by tailoring the support membrane structure, modifying the support membrane chemistry and optimizing the interfacial polymerization conditions.

In this work we have combined two processes with the objective of obtaining the best results in the treatment of brackish waters. Initially, the filtration process to evaluate the membranes in terms of water permeability and subsequently the FO process to assess the ability of the membrane to reject salt. However, the combination of these processes could be performed in reverse: first the system FO which uses a semi-permeable membrane to reject salts, super hydrophilic nanoparticles as draw solutes to induce water across the FO membrane, and after that, the UF process in which the membranes are used to regenerate the draw solutes without increasing nano-particle size or reducing osmotic functionality. UF membranes of small

pore diameter and narrow pore size distribution can enhance the recovery efficiency of nanoparticle draw solution.

In principle, using small molecules, salts and electrolytes may not be economical and practical because of the difficulties of recovery and salt leakage, in addition to inducing clogging in the supporting layer and resulting in severe fouling and internal concentration polarization [103]. The use of FO with the aid of membrane distillation (MD) appears to be a better idea [104]. However, MD is not a commercially available technology even after 30 years of study. The required low-quality or low-cost heat for MD is essential but cannot be easily found in a practical sense. In addition, the fouling including scaling and crystallization in MD is another issue. Using highly hydrophilic nano-particles as draw solutes may be one of the solutions to overcome the above issues. [9]

7 References

[1] H.Y. Ng, W. Tang, W.S. Wong, Performance of forward (direct) osmosis process: Membrane structure and transport phenomenon, Environmental Science and Technology 40 (2006) 2408-2413.

[2] B.B. Alfred, W.D. Eric, W. Donald, Ion-exchange resins (1972) US3645922 A.

[3] H.F. Walton, Ion Exchange, Science 138 (1962) 133.

[4] P. Simon, Tapped Out: The Coming World Crisis in Water and What We Can Do About It, (2001) Welcome Rain Publishers.

[5] R.W. Baker, Membrane Technology and Applications, (2012) Wiley, California.

[6] T. Humplik, J. Lee, S.C. O'Hern, B.A. Fellman, M.A. Baig, S.F. Hassan, M.A. Atieh, F. Rahman, T. Laoui, R. Karnik, E.N. Wang, Nanostructured materials for water desalination, Nanotechnology 22 (2011) 292001.

[7] P.W.B. M.A. Shannon, M. Elimelech, J.G. Georgiadis, B.J. Mariñas, A.M. Mayes, Anne M., Science and technology for water purification in the coming decades, Nature 452 (2008) 301–310.

[8] C. Suh, S. Lee, Modeling reverse draw solute flux in forward osmosis with external concentration polarization in both sides of the draw and feed solution, Journal of Membrane Science 427 (2013) 365-374.

[9] T.-S. Chung, S. Zhang, K.Y. Wang, J. Su, M.M. Ling, Forward osmosis processes: Yesterday, today and tomorrow, Desalination 287 (2012) 78-81.

[10] D. Emadzadeh, W.J. Lau, A.F. Ismail, Synthesis of thin film nanocomposite forward osmosis membrane with enhancement in water flux without sacrificing salt rejection, Desalination 330 (2013) 90-99.

[11] V. Yangali-Quintanilla, Z. Li, R. Valladares, Q. Li, G. Amy, Indirect desalination of Red Sea water with forward osmosis and low pressure reverse osmosis for water reuse, Desalination 280 (2011) 160-166.

[12] C.Y. Tang, Q. She, W.C.L. Lay, R. Wang, A.G. Fane, Coupled effects of internal concentration polarization and fouling on flux behavior of forward osmosis membranes during humic acid filtration, Journal of Membrane Science 354 (2010) 123-133.

[13] G.T. Gray, J.R. McCutcheon, M. Elimelech, Internal concentration polarization in forward osmosis: role of membrane orientation, Desalination 197 (2006) 1-8.

[14] J.R. McCutcheon, M. Elimelech, Modeling water flux in forward osmosis: Implications for improved membrane design, AIChE Journal 53 (2007) 1736-1744.

[15] M. Hu, B. Mi, Enabling graphene oxide nanosheets as water separation membranes, Environmental Science and Technology 47 (2013) 3715-3723.

[16] M.R. Dalwani, Thin film composite nanofiltration membranes for extreme conditions (2011) Doctoral Dissertation, University of Twente, The Netherlands

[17] C. Kong, T. Shintani, T. Tsuru, "Pre-seeding"-assisted synthesis of a high performance polyamide-zeolite nanocomposite membrane for water purification, New Journal of Chemistry 34 (2010) 2101-2104.

[18] S.H. Maruf, D.U. Ahn, J. Pellegrino, J.P. Killgore, A.R. Greenberg, Y. Ding, Correlation between barrier layer Tg and a thin-film composite polyamide membrane's performance: Effect of chlorine treatment, Journal of Membrane Science 405–406 (2012) 167-175.

[19] W.J. Koros, R. Mahajan, Pushing the limits on possibilities for large scale gas separation: which strategies?, Journal of Membrane Science 181 (2001) 141.

[20] M.G. Süer, N. Baç, L. Yilmaz, Gas permeation characteristics of polymer-zeolite mixed matrix membranes, Journal of Membrane Science 91 (1994) 77-86.

[21] L.M. Pastrana-Martínez, S. Morales-Torres, S.K. Papageorgiou, F.K. Katsaros, G.E. Romanos, J.L. Figueiredo, J.L. Faria, P. Falaras, A.M.T. Silva, Photocatalytic behaviour of nanocarbon–TiO_2 composites and immobilization into hollow fibres, Applied Catalysis B: Environmental 142–143 (2013) 101-111.

[22] S. Morales-Torres, T.L.S. Silva, L.M. Pastrana-Martinez, A.T.S.C. Brandao, J.L. Figueiredo, A.M.T. Silva, Modification of the surface chemistry of single- and multi-walled carbon nanotubes by HNO_3 and H_2SO_4 hydrothermal oxidation for application in direct contact membrane distillation, Physical Chemistry Chemical Physics 16 (2014) 12237-12250.

[23] L.M. Pastrana-Martínez, S. Morales-Torres, V. Likodimos, P. Falaras, J.L. Figueiredo, J.L. Faria, A.M.T. Silva, Role of oxygen functionalities on the synthesis of photocatalytically active graphene–TiO2 composites, Applied Catalysis B: Environmental 158–159 (2014) 329-340.

[24] J. Chen, A.M. Rao, S. Lyuksyutov, M.E. Itkis, M.A. Hamon, H. Hu, R.W. Cohn, P.C. Eklund, D.T. Colbert, R.E. Smalley, R.C. Haddon, Dissolution of full-length single-walled carbon nanotubes, Journal of Physical Chemistry B 105 (2001) 2525-2528.

[25] O.V. Prezhdo, P.V. Kamat, G.C. Schatz, Virtual issue: Graphene and functionalized graphene, Journal of Physical Chemistry C 115 (2011) 3195-3197.

[26] D.R. Dreyer, S. Park, C.W. Bielawski, R.S. Ruoff, The chemistry of graphene oxide, Chemical Society Reviews 39 (2010) 228-240.

[27] A.M.T. Association, Water Desalination Processes (2007) Available from: http://www.amtaorg.com/wp-content/uploads/8_WaterDesalinationProcesses.pdf

[28] R. Semiat, D. Hasson, Water Desalination, Reviews in Chemical Engineering 28 (2012) 43-60.

[29] A.T.S.C. Brandão, Membranes with nanostructured carbon materials for water desalination and purification (2013) Master's Thesis in Chemical Engineering Universidade do Porto, Portugal.

[30] J.A. Nollet, Lecons de physique experimentale, (1748) Du fonds de H.L Guerin & L.F. Delatour, Paris.

[31] M.I.G. Monteiro, Forward osmosis membranes tailored by hydrogel coatings (2012) Master's Thesis in Chemical and Biochemical Engineering, Universidade Nova de Lisboa, Portugal.

[32] S. Zhao, L. Zou, C.Y. Tang, D. Mulcahy, Recent developments in forward osmosis: Opportunities and challenges, Journal of Membrane Science 396 (2012) 1-21.

[33] T.Y. Cath, A.E. Childress, M. Elimelech, Forward osmosis: Principles, applications, and recent developments, Journal of Membrane Science 281 (2006) 70-87.

[34] E.D. Manev, K.H. Kolikov, I.L. Minkov, B.P. Radoev, Modeling of osmotic kinetics in aqueous solutions, based on experimental data, Colloids and Surfaces A: Physicochemical and Engineering Aspects *In press* (2014) doi: 10.1016/j.colsurfa.2014.1001.1006.

[35] J.T. Moore, Colligative Properties for AP Chemistry (2011) Available from: http://www.education.com/study-help/article/colligative-properties/

[36] M. Mulder, Basic Principles of Membrane Technology, (1996) Kluwer Academic Publishers, The Netherlands.

[37] W.C.L. Lay, J. Zhang, C. Tang, R. Wang, Y. Liu, A.G. Fane, Factors affecting flux performance of forward osmosis systems, Journal of Membrane Science 394–395 (2012) 151-168.

[38] S. Zhao, L. Zou, Relating solution physicochemical properties to internal concentration polarization in forward osmosis, Journal of Membrane Science 379 (2011) 459-467.

[39] A. Achilli, T.Y. Cath, A.E. Childress, Power generation with pressure retarded osmosis: An experimental and theoretical investigation, Journal of Membrane Science 343 (2009) 42-52.

[40] Y. Xu, X. Peng, C.Y. Tang, Q.S. Fu, S. Nie, Effect of draw solution concentration and operating conditions on forward osmosis and pressure retarded osmosis performance in a spiral wound module, Journal of Membrane Science 348 (2010) 298-309.

[41] M.C.Y. Wong, K. Martinez, G.Z. Ramon, E.M.V. Hoek, Impacts of operating conditions and solution chemistry on osmotic membrane structure and performance, Desalination 287 (2012) 340-349.

[42] J. Su, T.-S. Chung, Sublayer structure and reflection coefficient and their effects on concentration polarization and membrane performance in FO processes, Journal of Membrane Science 376 (2011) 214-224.

[43] L. Liu, M. Wang, D. Wang, C. Gao, Current Patents of Forward Osmosis Membrane Process, Recent Patents on Chemical Engineering 2 (2009) 76-82.

[44] Q. Ge, J. Su, G.L. Amy, T.-S. Chung, Exploration of polyelectrolytes as draw solutes in forward osmosis processes, Water Research 46 (2012) 1318-1326.

[45] M. Elimelech, W.A. Phillip, The Future of Seawater Desalination: Energy, Technology, and the Environment, Science 333 (2011) 712-717.

[46] M.E. R.L. McGinnis, Global challenges in energy and water supply: the promise of engineered osmosis, Environmental Science & Technology 42 (2008) 8625–8629.

[47] R.L. McGinnis, M. Elimelech, Energy requirements of ammonia–carbon dioxide forward osmosis desalination, Desalination 207 (2007) 370-382.

[48] A. Achilli, T.Y. Cath, E.A. Marchand, A.E. Childress, The forward osmosis membrane bioreactor: A low fouling alternative to MBR processes, Desalination 239 (2009) 10-21.

[49] B. Mi, M. Elimelech, Organic fouling of forward osmosis membranes: Fouling reversibility and cleaning without chemical reagents, Journal of Membrane Science 348 (2010) 337-345.

[50] M.E. B. Mi, Gypsum scaling and cleaning in forward osmosis: measurements and mechanisms, Environmental Science & Technology 44 (2010) 2022–2028.

[51] S. Lee, C. Boo, M. Elimelech, S. Hong, Comparison of fouling behavior in forward osmosis (FO) and reverse osmosis (RO), Journal of Membrane Science 365 (2010) 34-39.

[52] J.R. McCutcheon, R.L. McGinnis, M. Elimelech, A novel ammonia—carbon dioxide forward (direct) osmosis desalination process, Desalination 174 (2005) 1-11.

[53] K.B. Petrotos, H.N. Lazarides, Osmotic concentration of liquid foods, Journal of Food Engineering 49 (2001) 201-206.

[54] Q. Yang, K.Y. Wang, T.-S. Chung, A novel dual-layer forward osmosis membrane for protein enrichment and concentration, Separation and Purification Technology 69 (2009) 269-274.

[55] B. Jiao, A. Cassano, E. Drioli, Recent advances on membrane processes for the concentration of fruit juices: a review, Journal of Food Engineering 63 (2004) 303-324.

[56] C.-Y. Wang, H.-O. Ho, L.-H. Lin, Y.-K. Lin, M.-T. Sheu, Asymmetric membrane capsules for delivery of poorly water-soluble drugs by osmotic effects, International Journal of Pharmaceutics 297 (2005) 89-97.

[57] J. Shokri, P. Ahmadi, P. Rashidi, M. Shahsavari, A. Rajabi-Siahboomi, A. Nokhodchi, Swellable elementary osmotic pump (SEOP): An effective device for delivery of poorly water-soluble drugs, European Journal of Pharmaceutics and Biopharmaceutics 68 (2008) 289-297.

[58] M.M. Pendergast, E.M.V. Hoek, A review of water treatment membrane nanotechnologies, Energy & Environmental Science 4 (2011) 1946-1971.

[59] R. Das, M.E. Ali, S.B.A. Hamid, S. Ramakrishna, Z.Z. Chowdhury, Carbon nanotube membranes for water purification: A bright future in water desalination, Desalination 336 (2014) 97-109.

[60] S. Judd, The MBR Book: Principles and Applications of Membrane Bioreactors for Water and Wastewater Treatment, (2011) Elsevier, Oxford.

[61] B.M. Ganesh, A.M. Isloor, A.F. Ismail, Enhanced hydrophilicity and salt rejection study of graphene oxide-polysulfone mixed matrix membrane, Desalination 313 (2013) 199-207.

[62] L.E.S. Brink, S.J.G. Elbers, T. Robbertsen, P. Both, The anti-fouling action of polymers preadsorbed on ultrafiltration and microfiltration membranes, Journal of Membrane Science 76 (1993) 281-291.

[63] K.J. Kim, A.G. Fane, C.J.D. Fell, The performance of ultrafiltration membranes pretreated by polymers, Desalination 70 (1988) 229-249.

[64] A. Higuchi, K. Sugiyama, B.O. Yoon, M. Sakurai, M. Hara, M. Sumita, S.-i. Sugawara, T. Shirai, Serum protein adsorption and platelet adhesion on pluronic™-adsorbed polysulfone membranes, Biomaterials 24 (2003) 3235-3245.

[65] Y. Yang, P. Wang, Q. Zheng, Preparation and properties of polysulfone/TiO_2 composite ultrafiltration membranes, Journal of Polymer Science Part B: Polymer Physics 44 (2006) 879-887.

[66] V. Vatanpour, S.S. Madaeni, R. Moradian, S. Zinadini, B. Astinchap, Novel antibifouling nanofiltration polyethersulfone membrane fabricated from embedding TiO_2 coated multiwalled carbon nanotubes, Separation and Purification Technology 90 (2012) 69-82.

[67] R.S. Ruoff, D.C. Lorents, Mechanical and thermal properties of carbon nanotubes, Carbon 33 (1995) 925-930.

[68] H.J.L. T.W.Ebbesen, H.Hiura,J.W.Bennett,H.F.Ghaemi,T.Thio, Electrical conductivity of individual carbon nanotubes, Nature 382 (1996) 54–56.

[69] J.-H. Choi, J. Jegal, W.-N. Kim, Fabrication and characterization of multi-walled carbon nanotubes/polymer blend membranes, Journal of Membrane Science 284 (2006) 406-415.

[70] V. Vatanpour, S.S. Madaeni, R. Moradian, S. Zinadini, B. Astinchap, Fabrication and characterization of novel antifouling nanofiltration membrane prepared from oxidized multiwalled carbon nanotube/polyethersulfone nanocomposite, Journal of Membrane Science 375 (2011) 284-294.

[71] E. Celik, H. Park, H. Choi, H. Choi, Carbon nanotube blended polyethersulfone membranes for fouling control in water treatment, Water Research 45 (2011) 274-282.

[72] Y. Xu, W. Hong, H. Bai, C. Li, G. Shi, Strong and ductile poly(vinyl alcohol)/graphene oxide composite films with a layered structure, Carbon 47 (2009) 3538-3543.

[73] J. Liang, Huang, Y., Zhang, L., Wang, Y., Ma, Y., Guo, T. and Chen, Y., Molecular-Level Dispersion of Graphene into Poly(vinyl alcohol) and Effective Reinforcement of their Nanocomposites, Advanced Functional Materials 19 (2009) 2297–2302.

[74] L.M. Pastrana-Martínez, S. Morales-Torres, V. Likodimos, J.L. Figueiredo, J.L. Faria, P. Falaras, A.M.T. Silva, Advanced nanostructured photocatalysts based on reduced graphene oxide–TiO_2 composites for degradation of diphenhydramine pharmaceutical and methyl orange dye, Applied Catalysis B: Environmental 123–124 (2012) 241-256.

[75] W.S. Hummers, R.E. Offeman, Preparation of Graphitic Oxide, Journal of the American Chemical Society 80 (1958) 1339-1339.

[76] D. Emadzadeh, W.J. Lau, T. Matsuura, M. Rahbari-Sisakht, A.F. Ismail, A novel thin film composite forward osmosis membrane prepared from PSf-TiO_2 nanocomposite substrate for water desalination, Chemical Engineering Journal 237 (2014) 70-80.

[77] G.R. Xu, J.N. Wang, C.J. Li, Strategies for improving the performance of the polyamide thin film composite (PA-TFC) reverse osmosis (RO) membranes: Surface modifications and nanoparticles incorporations, Desalination 328 (2013) 83-100.

[78] S. Brunauer, P.H. Emmett, E. Teller, Adsorption of gases in multimolecular layers, Journal of the American Chemical Society 60 (1938) 309-319.

[79] J.R.F. Rouquerol, K. Sing, Adsorption by Powders and Porous Solids, (1999), London.

[80] D. Hopkinson, M. Zeh, D. Luebke, The bubble point of supported ionic liquid membranes using flat sheet supports, Journal of Membrane Science 468 (2014) 155-162.

[81] J. Yu, X. Hu, Y. Huang, A modification of the bubble-point method to determine the pore-mouth size distribution of porous materials, Separation and Purification Technology 70 (2010) 314-319.

[82] J.L. Figueiredo, M.F.R. Pereira, M.M.A. Freitas, J.J.M. Órfão, Modification of the surface chemistry of activated carbons, Carbon 37 (1999) 1379-1389.

[83] J.L. Figueiredo, M.F.R. Pereira, M.M.A. Freitas, J.J.M. Órfão, Characterization of Active Sites on Carbon Catalysts, Industrial & Engineering Chemistry Research 46 (2007) 4110-4115.

[84] P. Pardeshi, A.A. Mungray, Synthesis, characterization and application of novel high flux FO membrane by layer-by-layer self-assembled polyelectrolyte, Journal of Membrane Science 453 (2014) 202-211.

[85] S. Morales-Torres, L.M. Pastrana-Martínez, J.L. Figueiredo, J.L. Faria, A.M.T. Silva, Graphene oxide-P25 photocatalysts for degradation of diphenhydramine pharmaceutical and methyl orange dye, Applied Surface Science 275 (2013) 361-368.

[86] R. Saranya, G. Arthanareeswaran, D.D. Dionysiou, Treatment of paper mill effluent using Polyethersulfone/functionalised multiwalled carbon nanotubes based nanocomposite membranes, Chemical Engineering Journal 236 (2014) 369-377.

[87] J.R. Ellerie, O.G. Apul, T. Karanfil, D.A. Ladner, Comparing graphene, carbon nanotubes, and superfine powdered activated carbon as adsorptive coating materials for microfiltration membranes, Journal of Hazardous Materials 261 (2013) 91-98.

[88] C.A. Crock, A.R. Rogensues, W. Shan, V.V. Tarabara, Polymer nanocomposites with graphene-based hierarchical fillers as materials for multifunctional water treatment membranes, Water Research 47 (2013) 3984-3996.

[89] K.M. Persson, V. Gekas, G. Trägårdh, Study of membrane compaction and its influence on ultrafiltration water permeability, Journal of Membrane Science 100 (1995) 155-162.

[90] K. Ebert, D. Fritsch, J. Koll, C. Tjahjawiguna, Influence of inorganic fillers on the compaction behaviour of porous polymer based membranes, Journal of Membrane Science 233 (2004) 71-78.

[91] M.T.M. Pendergast, J.M. Nygaard, A.K. Ghosh, E.M.V. Hoek, Using nanocomposite materials technology to understand and control reverse osmosis membrane compaction, Desalination 261 (2010) 255-263.

[92] N.A.A. Hamid, A.F. Ismail, T. Matsuura, A.W. Zularisam, W.J. Lau, E. Yuliwati, M.S. Abdullah, Morphological and separation performance study of polysulfone/titanium dioxide (PSF/TiO2) ultrafiltration membranes for humic acid removal, Desalination 273 (2011) 85-92.

[93] A. Mills, S. Le Hunte, An overview of semiconductor photocatalysis, Journal of Photochemistry and Photobiology A: Chemistry 108 (1997) 1-35.

[94] S.H. Kim, S.-Y. Kwak, B.-H. Sohn, T.H. Park, Design of TiO_2 nanoparticle self-assembled aromatic polyamide thin-film-composite (TFC) membrane as an approach to solve biofouling problem, Journal of Membrane Science 211 (2003) 157-165.

[95] R. Jiraratananon, A. Sungpet, P. Luangsowan, Performance evaluation of nanofiltration membranes for treatment of effluents containing reactive dye and salt, Desalination 130 (2000) 177-183.

[96] R.J. Petersen, Composite reverse osmosis and nanofiltration membranes, Journal of Membrane Science 83 (1993) 81-150.

[97] C. Kim, S. Lee, H.K. Shon, M. Elimelech, S. Hong, Boron transport in forward osmosis: Measurements, mechanisms, and comparison with reverse osmosis, Journal of Membrane Science 419–420 (2012) 42-48.

[98] J. Wei, X. Liu, C. Qiu, R. Wang, C.Y. Tang, Influence of monomer concentrations on the performance of polyamide-based thin film composite forward osmosis membranes, Journal of Membrane Science 381 (2011) 110-117.

[99] N.Y. Yip, A. Tiraferri, W.A. Phillip, J.D. Schiffman, M. Elimelech, High Performance Thin-Film Composite Forward Osmosis Membrane, Environmental Science & Technology 44 (2010) 3812-3818.

[100] E.R. Cornelissen, D. Harmsen, K.F. de Korte, C.J. Ruiken, J.-J. Qin, H. Oo, L.P. Wessels, Membrane fouling and process performance of forward osmosis membranes on activated sludge, Journal of Membrane Science 319 (2008) 158-168.

[101] V.M.M. Lobo, Mutual diffusion coefficients in aqueous electrolyte solutions (Technical Report), Pure and Applied Chemistry 65 (1993) 2613.

[102] M. Qasim, Performance of Forward Osmosis Using Various Membranes (2013) Master's Thesis in Science in Chemical Engineering, American University of Sharjah, United Arab Emirates.

[103] N.T. Hancock, T.Y. Cath, Solute Coupled Diffusion in Osmotically Driven Membrane Processes, Environmental Science & Technology 43 (2009) 6769-6775.

[104] C.R. Martinetti, A.E. Childress, T.Y. Cath, High recovery of concentrated RO brines using forward osmosis and membrane distillation, Journal of Membrane Science 331 (2009) 31-39.